photonics

MDPI

Article

Multimode Optical Fiber Materials for Enhanced Mode Conversion and Holographic Reconstruction Using Machine Learning and Spatial Division Multiplexing

Hanwen Zhao

Department of Electronic and Electrical Engineering, University College London (UCL), London WC1E 6BT, UK; sdnyzhw@outlook.com

Abstract

With the growing need for high-density data and real-time communication, multimode optical fibers (MMFs) have emerged as a vital technology due to their ability to transmit multiple optical modes simultaneously through spatial division multiplexing (SDM). However, issues such as mode coupling and dispersion continue to compromise signal clarity. This study presents a quantitative analysis of machine learning applications for enhancing mode conversion and holographic reconstruction in MMF systems. We demonstrate that a shallow artificial neural network can predict reconstruction accuracy, information transfer capacity, and adaptive system efficiency based on mode coupling and dispersion inputs, achieving prediction errors below 4% on case-study data. A convolutional neural network achieves 93.7% accuracy for mode separation, with a 62% reduction in mode error rate compared to conventional reconstruction methods. Hybrid physics-informed learning approaches incorporating energy conservation and phase stability constraints are explored, showing promise for improved generalization. Our results indicate that machine learning significantly enhances reconstruction precision and information transmission in MMFs, providing a foundation for next-generation communication and imaging systems. Despite certain training challenges, these models effectively process complex data, demonstrating their reliability and predictive capabilities.

Keywords: multimode optical fibers (MMFs); machine learning; holographic reconstruction; deep learning; data transmission; spatial division multiplexing

1. Introduction

In recent years, the escalating demand for higher bandwidth and more accurate imaging in optical systems has driven the adoption of multimode optical fibers (MMFs) as a platform for transmitting large amounts of information. Unlike single-mode fibers (SMFs), which support only one optical path, MMFs can carry multiple optical modes simultaneously, offering the potential to exploit spatial parallelization [1–4]. However, a fundamental challenge in using MMFs arises from the complex nature of intermode coupling, scattering phenomena, and environmental sensitivities that distort light propagation along the fiber. These issues necessitate advanced methods for analyzing and retrieving optical modes. Machine learning (ML), particularly deep learning, provides powerful tools for modeling complex relationships and extracting patterns from noisy data [5–7]. Integrating these algorithms into optical system design—especially for mode conversion and holographic imaging via MMFs—promises significant gains in accuracy and efficiency [6–8]. This paper

Check for updates

Received: 17 May 2026
Revised: 17 July 2026
Accepted: 20 July 2026
Published: 29 July 2026

Copyright: © 2026 by the author. Licensee MDPI, Basel, Switzerland. This article is an open access article distributed under the terms and conditions of the Creative Commons Attribution (CC BY) license.

focuses on achieving real-time holography, high-resolution imaging, and secure, fast data transmission by combining Space Division Multiplexing (SDM) and ML techniques. We discuss fundamental concepts, review prior studies, analyze reported methods and results, and explore future perspectives [9–11].

The exponential growth in demand for high-speed, high-capacity data transmission—driven by cloud computing, the Internet of Things (IoT), artificial intelligence (AI), and augmented reality—has placed optical communication technologies at the forefront [10–14]. Nevertheless, MMFs, as a transformative platform for increasing communication capacity via SDM, have revolutionized optical network architectures. MMFs provide multiple simultaneous spatial paths through a single core, enabling multiple independent information channels [15,16]. Yet, practical MMF use is hindered by mode coupling and intermodal dispersion [3–6]. Due to physical inhomogeneities, thermal distortions, bending, or refractive index fluctuations, different light modes interact strongly along the fiber, causing interference and information attenuation—posing serious challenges for original signal reconstruction. Hence, precise mode conversion and recovery methods are essential for controlling light propagation in MMFs [3,4].

Optical holography, one of the most advanced methods for 3D scene imaging and reconstruction, is increasingly moving toward fiber-based implementations. Holography's ability to record phase and spatial information is invaluable for medicine, digital microscopy, mixed reality, and quantum communications. However, effective holography within MMFs requires accurate reconstruction of complex wave patterns and interference phases that become severely disturbed during fiber transmission. At this juncture, ML—especially deep learning—emerges as a powerful tool for modeling nonlinear and complex systems. Deep neural networks such as convolutional neural networks (CNNs), autoencoders, and generative adversarial networks (GANs) can learn hidden patterns and internal dynamics that are not easily modeled by traditional methods. In the context of MMFs, these algorithms play a vital role in prediction, reconstruction, noise filtering, and adaptive control of light transmission. CNNs, with their spatial and temporal feature extraction capabilities, can transform the fiber's output image back into its original features, enabling accurate optical pattern reconstruction. Autoencoders create compact representations of large data volumes from MMF outputs for mode conversion or classification. GANs excel at reconstructing complex holographic images, especially under noisy or incomplete data conditions [5–8].

At a more advanced level, reinforcement learning has been proposed for active control systems that regulate transmission dynamics within the fiber, responding to environmental changes in real time while maintaining performance amid physical noise and dynamic fluctuations. Additionally, Transformer networks—originally designed for natural language processing—have recently succeeded in photonics, particularly for analyzing sequential and long-term dependencies of optical properties along the fiber [9–11]. Experimentally, laboratories equipped with wavefront sensing, interferometry, and fast imaging tools now enable collection of real-world MMF data for training learning models. This integration of physical and computational worlds has created a highly dynamic interdisciplinary field at the intersection of photonics, ML, and intelligent distributed systems [12,13].

Theoretically, light propagation in MMFs can be formulated via Maxwell's equations and numerical models like finite-difference time-domain (FDTD) or transfer matrix methods (TMMs). However, these approaches face serious limitations at operational and real-time scales due to high numerical complexity, sensitivity to boundary conditions, and strong dependence on the fiber's physical structure. ML algorithms offer an alternative or complementary solution: data-driven modeling of fiber behavior without requiring detailed knowledge of its physical structure. These models identify hidden patterns in mode coupling, phase perturbations, and intermode interference using experimental or simulated

data and then use them to predict or reconstruct input modes [14]. From an information theory perspective, SDM in MMFs is equivalent to opening parallel channels in mode space, theoretically multiplying system information capacity. However, complex dependence between these channels—arising from mode interactions—requires sophisticated signal processing methods capable of separating and isolating modes under noisy and unstable conditions. ML algorithms with distributed and memory-based learning capabilities (e.g., LSTMs or Transformers) are well-suited for such systems with complex temporal dynamics and spatial delays, as they can identify long-term dependencies between fiber input and output for signal reconstruction [15].

An emerging trend is hybrid learning, where physics-informed learning is combined with experimental data. This approach mitigates limitations due to scarce labeled data and enhances model generalizability across different scenarios. For instance, incorporating physical constraints—such as energy conservation, phase stability, or spatial continuity—into the learning model's cost function ensures outputs are both numerically and physically meaningful. From an implementation perspective, integrating learning algorithms with optoelectronic hardware (e.g., photonic chips) can lead to all-optical systems with local decision-making and processing capabilities. Concepts such as neural optical computing and photonic neuromorphic systems are becoming active research streams, reducing processing latency and energy consumption while providing suitable platforms for edge computing in applications like the optical Internet of Things [16,17].

This study addresses three specific research questions: (RQ1) How do mode coupling and intermode dispersion quantitatively affect holographic reconstruction accuracy, as measured by structural similarity index and mode error rate? (RQ2) Can CNN-based approaches achieve superior mode separation compared to traditional digital signal processing methods, including Fourier reconstruction and iterative phase retrieval? (RQ3) Do physics-informed learning strategies incorporating physical constraints improve model generalization across varying operational conditions, specifically temperature variations from 15 °C to 45 °C?

This article is structured as an original research contribution that combines experimental measurements, physics-based simulations, and machine learning analysis. Our work is organized around three core pillars: (i) quantitative analysis of MMF parameter interactions using ANN modeling, (ii) CNN-based mode separation with comparative evaluation against non-ML methods, and (iii) exploration of physics-informed learning strategies for enhanced holographic reconstruction. The results presented are original unless explicitly cited as literature-based, and all simulated data are clearly distinguished from experimental measurements throughout the manuscript.

While earlier research has often treated MMF propagation challenges and ML-based reconstruction as separate issues, this study provides a quantitative framework for understanding how key optical parameters interact and evaluates ML approaches using a combined experimental and simulated dataset. Second, we evaluate how well a convolutional neural network (CNN) performs mode separation under noisy conditions, achieving over 95% accuracy and a 30% lower mode error rate compared to baseline methods. Third, we explore hybrid physics-informed machine learning approaches that embed physical constraints—such as energy conservation and phase stability—directly into the learning models. These hybrid models offer better generalization and resilience, performing reliably across temperature variations from 15 °C to 45 °C and under electromagnetic noise as low as 10 dB SNR. Together, these findings deepen our understanding of parameter interactions in MMF systems and lay the groundwork for designing smarter optical systems for high-capacity communications and holographic imaging.

2. Physical Properties of Optical Fibers

Optical fibers for MMF applications are primarily fabricated from high-purity silica glass (SiO_2) with controlled refractive index profiles. The core region is typically doped with germanium dioxide (GeO_2) to increase the refractive index relative to the pure silica cladding, enabling total internal reflection. For graded-index MMFs, the refractive index follows a parabolic profile achieved through controlled doping gradients. The material composition directly affects key propagation parameters, including attenuation (typically 0.2–3 dB/km depending on wavelength), nonlinear coefficients, and thermal stability. These material properties are fundamental to understanding mode coupling, dispersion, and the overall system performance analyzed in this study.

2.1. Multimode Fiber (MMF)

The material properties of optical fibers fundamentally determine their propagation characteristics and influence the performance of machine learning-based reconstruction methods. Understanding these physical properties is essential for interpreting the experimental results presented in this study. Multimode fibers are capable of simultaneously transmitting multiple independent optical modes. These modes can be spatially, temporally, or frequency-separated. MMF is one of the key structures in optical data transmission that provides the ability to transmit multiple spatial optical modes simultaneously in a single fiber core. MMFs are engineered to transmit multiple light modes simultaneously and are primarily composed of silica, which provides excellent optical properties. The larger core diameter facilitates the propagation of various light paths. Chemically, the core can be doped with materials such as germanium to modify its refractive index, enhancing light transmission efficiency and signal integrity. The surrounding cladding, typically made from lower-refractive-index silica, ensures total internal reflection, effectively confining light within the core. Unlike SMFs that transmit only one fundamental optical mode, MMFs can carry multiple discrete light modes, each with its own electromagnetic field distribution, in parallel. This feature makes MMFs play a fundamental role in high-capacity data transmission, optical imaging, and optical holography [18,19].

MMFs consist of three main components: the core, cladding, and coating. The core, which has a higher refractive index, guides light and typically has a diameter ranging from 50 to 100 μm, in contrast to SMFs that measure about 8 to 10 μm. Surrounding the core is the cladding, a lower-refractive-index layer that facilitates total internal reflection, keeping the light contained within the core. The outermost layer, known as the coating, provides mechanical and thermal protection. MMFs can be categorized based on their refractive index characteristics and mode support into two main types: step-index MMFs, where the refractive index in the core changes abruptly compared to the cladding, resulting in high intermodal dispersion but easier manufacturing, and graded-index MMFs, which feature a continuously decreasing refractive index from the core center to the cladding, significantly reducing intermodal dispersion and enhancing data transmission speed.

Scalability in optical networks is crucial for accommodating the ever-increasing demand for bandwidth and connectivity. As data traffic continues to grow exponentially, network architectures must evolve to support higher capacities without compromising performance. Real-world optical networks leverage advanced technologies such as wavelength division multiplexing (WDM) and dense wavelength division multiplexing (DWDM) to maximize the use of existing fiber infrastructure. A scalable optical network can efficiently expand by adding more wavelengths or channels, enabling operators to meet customer demands without extensive overhauls. Flexibility is also essential; networks must adapt to various applications, from data centers to long-haul transmissions. Moreover, software-defined networking (SDN) plays a pivotal role in scalability, allowing for dynamic

resource allocation and network management. Automated provisioning and reconfiguration capabilities enhance operational efficiency, enabling rapid deployment of new services. Incorporating artificial intelligence and ML can further optimize network performance and predict traffic patterns, ensuring that resources are allocated efficiently. Scalable optical networks not only support current needs but also future-proof infrastructures, paving the way for innovations such as 5G and beyond, ensuring robust, high-speed connectivity in increasingly digital societies.

Fibers that support only a limited number of modes (e.g., 4 to 6 modes) lie between SMFs and MMFs and are suitable for controlled SDM [20–24]. Light transmission in MMFs is analyzed by solving Maxwell's wave equation for cylindrical media. The allowed modes of the electromagnetic field are defined as Helmholtz modes, and the allowed modes are determined based on the boundary conditions between the core and cladding. These modes consist of combinations of Bessel and Neumann functions in cylindrical geometry. In general, the benefits and challenges can be as follows. MMFs offer several advantages, including high data transfer capacity through spatial parallelization, lower manufacturing costs compared to SMFs for short-range applications, and versatility in various fields, such as imaging, microscopy, holography, and local area networks. However, they also face challenges, including intermodal dispersion, where different modes propagate at varying speeds, causing pulse stretching; mode coupling, which disrupts the original signal structure; attenuation and phase distortion from long-distance mode propagation; and sensitivity to environmental changes like bending, temperature fluctuations, and vibrations. MMFs are applied in multiple areas: they enhance optical communications with SDM, increasing transmission capacity significantly; serve as flexible optical lenses in imaging and microscopy, particularly in inaccessible locations; facilitate digital holography by requiring accurate phase reconstruction for 3D holograms; and are utilized in the design of optical sensors for monitoring temperature, pressure, and strain due to their high sensitivity to environmental changes.

2.1.1. Theoretical Framework for Mode Coupling

Mode coupling in MMFs is governed by the coupled-mode equations. For a fiber supporting N modes, the propagation of the electric field E(z,t) can be expressed as

$$\partial E_n/\partial z = -j\beta_n E_n + \Sigma_{m\neq n} \kappa_{nm} E_m$$

where β_n is the propagation constant of mode n, and κ_{nm} is the coupling coefficient between modes n and m. The coupling coefficient κ_{nm} depends on the fiber perturbation, which can be expressed as

$$\kappa_{nm} = (\omega/4) \iint \Delta\varepsilon(x,y,z)\, e_n \cdot e_m^* \, dxdy$$

where $\Delta\varepsilon$ represents the permittivity perturbation due to fiber imperfections, and e_n and e_m are the modal field distributions.

2.1.2. Dispersion Analysis

Intermode dispersion $\Delta\tau$ arises from the differential group delay between modes:

$$\Delta\tau = L \times (1/v_{g,m} - 1/v_{g,n})$$

where $v_{g,m} = d\omega/d\beta_m$ is the group velocity of mode m, and L is the fiber length. The group velocity dispersion (GVD) for each mode is given by

$$D_m = -(2\pi c/\lambda^2)(d^2\beta_m/d\omega^2)$$

For graded-index MMFs optimized for minimal modal dispersion, the refractive index profile is as follows:

$$n(r) = n_1 \left[1-2\Delta(r/a)^{\alpha}\right]^{1/2}$$

where $\alpha \approx 2$ minimizes intermode dispersion by compensating for the dispersion of different modes. However, imperfections cause deviations from this ideal profile, leading to the residual dispersion analyzed in this study.

2.2. Space Division Multiplexing (SDM)

SDM is a technique for increasing data transmission capacity by using multiple independent spatial channels. In MMFs, these channels are implemented as different mode states. SDM, as one of the most advanced methods for increasing capacity in optical data transmission systems, has found a special place in the development of high-speed networks and future-oriented communication infrastructures in recent years. The main idea in SDM is to use the spatial degree of freedom in light to transmit multiple independent information streams in parallel over a common physical medium [25–27]. Unlike traditional methods such as wavelength division multiplexing (WDM), time division multiplexing (TDM), or polarization division multiplexing (PDM), which increase transmission capacity by using spectral or temporal properties of the signal, SDM exploits the spatial and topological properties of the electromagnetic field to transmit data channels simultaneously, but separately, along an optical path [28–31]. In the optical fiber context, SDM is usually implemented in two main ways: using MMFs or multicore fibers (MCF). In the first case, the different modes of light that can be supported in multimode fibers act as separate transmission paths, and each mode is considered an independent communication channel. In the second case, each core in a multicore fiber is considered a physical transmission path by itself. The use of SDM in these areas can increase data transmission capacity by several tens, without the need to increase the spectral bandwidth, which in many cases is limited physically or by regulations [32]. From a physical point of view, the optical modes in multimode fibers are a function of the distribution of the electromagnetic field in the fiber cross-section. These modes, which can be solved as eigenfunctions of Maxwell's equations for the cylindrical structure of the fiber, have different propagation properties, including group velocity, dispersion coefficient, and phase distribution. These differences cause the modes to interact with the medium in different ways along the path, and therefore, for optimal use of SDM, there is a need to convert, separate, and precisely control these modes. These tasks are usually performed by components such as Mode Multiplexer/Demultiplexer, Mode Converter, and Mode Filter, the design and manufacture of which require high optical and engineering precision [33]. One of the biggest challenges of SDM, especially in multimode fibers, is the phenomenon of intermodal coupling, which causes different signals transmitted through different modes to interfere with each other in an unwanted way. This phenomenon is caused by random disturbances in the fiber structure, thermal distortions, or even mechanical bending along the transmission path. Intermodal dispersion also leads to time stretching and phase distortion of signals, which, if not compensated, will cause intersymbol interference (ISI) and reduce the data transfer rate. Here, the use of digital signal processing (DSP) algorithms and, in particular, ML-based modeling plays a key role in compensating and controlling these effects [34].

At the system level, SDM-based architectures are being developed for use in data centers, sixth-generation (6G) networks, and quantum communication systems. In such applications, the ability to simultaneously transmit multiple video streams, sensor data, or quantum signals over a single optical fiber will lead to significant savings in cost, energy, and physical space. In particular, in the field of optical holography, SDM plays a key role in providing high-resolution phase image transmission infrastructures, because each mode can

transmit information related to a specific angle or view of the holographic image, and their combination at the destination allows for 3D reconstruction of the image. In recent years, extensive research has been initiated to utilize deep neural networks to model the complexities of SDM. These networks can identify the existing modes based on the output image of the fiber, model the coupling effects, and implement signal correction and reconstruction solutions at the destination using methods such as supervised or reinforcement learning. Combining SDM with ML has opened new horizons for real-time telecommunication systems, advanced optical imaging, and environmental analytics. Spatial parallelization thus represents both a technological advance and a conceptual framework for maximizing the information-carrying capacity of optical fibers [35].

2.3. Mode Conversion

Mode conversion is the process by which light emitted in one mode from an optical fiber or waveguide is converted to another mode in a controlled and targeted manner. This process is at the heart of MMF technologies, particularly in areas such as spatial demultiplexing (SDM), advanced optical holography, and ML-based optical signal processing, and is an essential tool for guiding, controlling, combining, and demultiplexing optical modes along the transmission path. From a physical perspective, optical modes in a fiber or waveguide are functions of the electromagnetic field that are solved in a particular form of Maxwell's wave equation in an inhomogeneous medium. These modes, which include different distributions of intensity, phase, polarization, and spatial structure of the light, each have distinct propagation properties, including cutoff frequency, group velocity, and cutoff wavelength. Mode conversion means the transfer of optical energy from one specific field function to another, without the energy disappearing or being scattered; rather, the goal is a precise and controlled change in the type of information-carrying mode. The mode conversion process can be performed in various ways. In its simplest form, a change in the waveguide structure (e.g., changing the radius or refractive index of the fiber) can induce coupling between the two modes and create the conversion. This conversion can be gradual and continuous, as occurs in tapered fibers or adiabatic mode converters, or abrupt and based on alternating structures, such as Bragg gratings and phase plates. In addition, the use of active optical elements such as optical modulators, metamaterial structures, and phase-matching mirrors also allows for controlled and dynamic mode conversion [36].

In multimode systems, especially those that utilize spatial parallelization, mode conversion plays a dual role: first, as a matching tool to prepare signals for entering or leaving optical channels; second, as a solution to compensate for disturbances caused by random coupling or intermode scattering. In this context, designing low-loss and robust mode converters against environmental distortions is a key engineering challenge. These advances, especially in the design of converters with adaptive frequency characteristics or high spatial modulation, have enabled the implementation of optical converters for real-time applications [37].

One of the critical applications of mode conversion is in the field of optical holography and multidimensional imaging. In this context, light with different mode structures (such as Laguerre–Gaussian or Hermite–Gaussian modes) carries information about the phase, depth, and spatial structure of the image. Accurate conversion of these modes before displaying or reconstructing the holographic image is essential for avoiding phase distortion and preserving 3D information. Also, in holographic systems with optical memory or rewritable holograms, mode conversion is used as an optical encoder. On the other hand, in interaction with ML, mode conversion plays the role of an intelligent intermediary for the connection between the input data and the spatial structure of light. In this application, environmental data or training signals are translated in a way that leads to the generation or

detection of specific modes of light. For example, trained CNNs can analyze light scattering structures and automatically determine the mode conversion required to reconstruct the original signal. Furthermore, in all-optical processing, the design of systems where mode conversion is equivalent to applying mathematical operations to the input data is becoming one of the forefront research lines in neurophotonics [38].

The main challenge in all these applications is to find a structure that can minimize losses and noise, maintain signal phase integrity, and accommodate high data rates. In response to this challenge, new concepts such as Mode-Aware Neural Networks, Photonic Reservoir Computing, and Mode-Selective Feedback are being developed, in which mode conversion acts not only as a transmission tool but also as a central processing element [39]. In general, state conversion in optical systems is not only a tool for data transmission but also a bridge between classical optical architecture and the future of adaptive and intelligent photonics; a tool that provides unprecedented capacities in light processing and transmission by utilizing quantum principles, learning algorithms, and nanoengineering [39].

2.4. Optical Holography

Optical holography is a 3D imaging technology that uses interference patterns of light to reconstruct scenes. In MMF-based systems, the main challenge is to accurately recover phase and spatial information. Optical holography is a fundamental branch of modern optics that is based on the recording and reconstruction of the complete information of a light wave, including amplitude and phase. Unlike conventional imaging, which only records light intensity, optical holography allows for three-dimensional, angular, and dynamic reconstruction of an object, opening the door to advanced technologies such as 3D displays, optical storage, nanophotonic sensors, and, more recently, ML-based optical data processing. At the core of optical holography, the interaction between two waves plays a key role: the reference beam and the object beam. When these two waves interfere on a recording surface such as a photosensitive plate or CMOS sensor, an interference pattern is formed that contains the complete phase and amplitude information of the object wave. This pattern is stored as a hologram. In the reconstruction step, re-irradiating the reference wave or a similar wave on this hologram reconstructs the object wave with all its spatial properties, such that the viewer can see a virtual or real three-dimensional image [40].

With the development of multimode fiber (MMF) technology and nanophotonic structures, the application of holography has expanded beyond an image recording method to areas such as optical encryption, wavefront shaping, and data transmission in spatial parallelization. In this regard, the ability to precisely control optical modes plays a crucial role, since different modes carry different information about the 3D image. For example, in a holographic system based on multimode fiber, higher-order modes may contain information related to depth or viewing angle, while the fundamental modes convey the overall view of the object. Therefore, designing systems that can achieve precise, stable, and controllable mode conversion is essential for accurate holographic reconstruction [41]. On the other hand, digital holography, which is based on recording hologram data by digital sensors and their numerical processing using numerical algorithms, has enabled the development of new reconstruction methods. In these methods, the reconstruction of the object wave is performed through algorithms such as Fourier reconstruction, phase transformation, spatio-spatial filtering, gradient algorithms, or ML. This approach has led to the rapid growth of holographic applications in noisy environments and biomedical and multimode systems. The integration of ML with holography is one of the most attractive research lines in modern photonics. In this approach, CNN or supervised learning models are trained to improve reconstruction accuracy, reduce noise, detect objects, or even

predict wavefront changes. Also, reinforcement learning can be used to find the best mode distribution for optimal image recording or reconstruction. In multimode holography, ML allows for mode detection and separation, compensation for distortion due to intermode scattering, and increased hologram resolution in dynamic environments. In addition, optical holography has been applied in high-density optical memories. Here, multiple holograms are simultaneously stored in a volume of material (Volume Holography), and each is read out at a different angle from the reference wave. This technology, with the help of SDM and mode conversion, has enabled the storage of large and multidimensional information in small substrates. Meanwhile, precise control of optical modes and the use of dedicated waveguides (such as waveguide holography) make it possible to optimize the storage and readout process [42]. In a macroscopic view, optical holography is no longer just a tool for imaging; it is also a new interface between photonics, data science, and quantum technologies. Shortly, the combination of holography with real-time light processing, optical computing, and distributed ML is expected to open new paths in human–machine interaction, biotechnology, and optical communications [43].

2.5. Machine Learning (ML)

Machine learning is performed by a set of algorithms that use data to learn patterns and make predictions or decisions. In this field, CNNs, recurrent networks (RNNs), and reinforcement learning (RL) are the most widely used. In recent years, significant advances in the field of ML, especially in the branches of deep learning and CNNs, have revolutionized the analysis of complex and nonlinear data. These advances play a vital and transformative role, especially in multimode optical systems that face the inherent complexities of optical modes, intermode scattering, and unwanted changes in the light path. Multimode optical systems are highly susceptible to signal distortion, mode coupling, and environmental noise due to the simultaneous propagation of multiple optical modes with different properties, which are very difficult and time-consuming to analyze using traditional methods. In these circumstances, ML algorithms with the ability to self-learn and extract key features from complex data enable accurate analysis and optimal reconstruction of modes [44,45]. The most significant applications of ML in the field of MMFs include several key areas. First, mode separation and identification are enhanced through CNNs trained on sample data, allowing for the recognition of complex spatiotemporal patterns and the separation of different modes in sparse data, which improves optical channel resolution and reduces intermode interference. Second, distorted signal reconstruction benefits from ML techniques, particularly recurrent neural networks (RNNs) and attention-based models, which can learn dynamic models of mode changes and correct distortions in real time, facilitating more accurate reconstruction of multimode optical signals. Additionally, reinforcement learning models enable the prediction and control of mode conversion, allowing systems to learn optimal conversion policies in complex environments and automatically adjust settings for improved data transmission. Noise reduction and hologram resolution enhancement are also achieved through advanced deep learning algorithms that effectively eliminate environmental noise from holographic data, significantly improving reconstruction resolution in multimode systems. Finally, real-time processing capabilities have been greatly advanced by parallel processing hardware such as GPUs and TPUs, enabling ML models to conduct real-time mode analysis and reconstruction, which supports interactive applications like dynamic holography and 3D displays.

The integration of ML with multimode optical systems not only effectively improves the quality of signal transmission and reconstruction but also provides a platform for the development of new technologies such as optical neural processing and optical quantum computing. These emerging fields, in which photonics and artificial intelligence are closely

intertwined, can lead to the enhancement of the capacity of telecommunication networks, the acceleration of computing, and the creation of self-organizing optical systems. The integration of ML with multimode optical systems provides a platform for enhanced signal reconstruction and transmission [45].

3. Materials and Methods

The limited experimental dataset (n = 225) revealed that model performance improves only modestly beyond 500 samples, motivating the exploration of transfer learning that leverages large simulated datasets with minimal experimental fine-tuning, while the observed 5% accuracy degradation at 45 °C, governed by $\Delta n = 1.1 \times 10^{-5}\ \Delta T$, underscores the need for real-time temperature monitoring integrated with ML prediction to enhance stability, and the CNN's 8.2% misclassification between LP11a and LP11b modes, arising from nearly identical propagation constants ($\Delta\beta \approx 0.05$ rad/m), calls for higher-order mode basis sets or alternative architectures to resolve this degeneracy, alongside the pressing need to reduce the current 28 ms inference time—which is borderline for real-time applications requiring <10 ms—through model quantization or FPGA-based hardware acceleration to achieve sub-5 ms latency [25–42]. To address these issues systematically, specific research directions include physics-guided data augmentation that enforces energy conservation and phase unwrapping to generate synthetic training data, potentially reducing experimental requirements by 60–70%; multi-task learning with a single network that simultaneously predicts reconstruction accuracy, mode composition, and dispersion characteristics to improve generalization and reduce overhead; real-time adaptive control using reinforcement learning, which already shows a 30% error reduction and should be optimized for response times under 1 ms for 10 Gb/s systems; integrated photonic–ML systems, where CNN convolutions are performed optically via photonic circuits, cutting energy consumption by 90% compared to GPUs and enabling edge-deployable ML-optimized MMF receivers; and multi-fiber generalization to systematically test trained models on fibers with different specifications—such as 62.5 μm core, step-index profiles, and varying dopant concentrations—building on the hybrid learning approach's promising 94% validation accuracy to ensure robust cross-fiber performance.

3.1. Advanced Photonics and ML

This study uses a combination of advanced photonic technology and ML algorithms to explore spatial parallelization, sophisticated mode conversion, and holographic reconstruction within MMF systems. The research is structured into two primary components, experimental and simulation, where critical parameters are meticulously controlled in both segments [36–38]. The utilized MMFs feature a 50 μm graded-index core, supporting the propagation of numerous optical modes, and are constructed from silica with a plastic coating to ensure thermal stability amid varying conditions. A semiconductor laser source emitting at 1550 nm, with an adjustable power of up to 20 mW, is employed, as this wavelength is optimal for minimizing attenuation in optical communications [37–41]. Mode conversion is achieved through Spatial Light Modulators (SLMs) and integrated photonic waveguide structures that can accurately generate complex modes, including Laguerre–Gaussian and Hermite–Gaussian modes. Holographic recording is performed using a digital system that incorporates a high-resolution CMOS camera (approximately 4 megapixels) capable of capturing interference patterns at 60 fps.

3.1.1. Optimizing Multimode Fiber Systems and Data Acquisition and Dataset Description

The implementation methods for this study involve several key steps. First, an MMF system is designed and set up, where a laser source illuminates the fiber under controlled

conditions with the aid of spatial converters. Different mode patterns are generated and precisely introduced into the fiber using Spatial Light Modulators (SLMs), allowing for initial measurements of mode interference, intermode coupling, and attenuation coefficients to inform subsequent analyses. Next, digital holograms are recorded and reconstructed; waves exiting the fiber are combined with a reference wave, and the resulting interference pattern is captured on a CMOS sensor. Through numerical processing utilizing Fourier and phase reconstruction algorithms, the hologram is reconstructed, extracting spatial and phase information related to the mode states. To further comprehend the behavior of various modes within the fiber, Zemax software is employed for light propagation modeling, defining the optical, geometric, and environmental parameters while simulating the effects of dispersion, mode coupling, and spatial distortions. The simulation results serve as training data for ML models. Deep CNNs are then implemented to analyze and reconstruct complex modes, with recorded holograms and simulation data used as input for training. Reinforcement learning algorithms enhance mode conversion and control mode coupling, while image preprocessing and resolution enhancement techniques are applied to reduce noise and improve reconstruction clarity. Finally, the performance of the mode reconstruction is evaluated by comparing ML results with experimental and simulation data, using qualitative metrics such as the structural similarity index (SSIM), mode error rate (MER), and signal-to-noise ratio (SNR) to assess accuracy. Sensitivity tests are conducted to evaluate model stability under varying temperatures, environmental noise, and parameter changes. This approach facilitates an in-depth investigation of mode behavior in MMFs and assesses the influence of environmental and equipment factors on system performance. By integrating experimental data, precise simulations, and ML, the methodology enhances system optimization and efficiency, providing a robust framework for complex multimode holographic applications and modern optical communication systems.

3.1.2. Artificial Neural Network (ANN) Modeling

This study used a shallow ANN as a proof-of-concept demonstration to explore relationships between input parameters (mode coupling and intermode dispersion) and output metrics (reconstruction accuracy, information transfer capacity, and real-time adaptive system efficiency). The network was trained using data from seven representative case-study samples, selected from the larger experimental dataset. While this limited sample size precludes claims of general predictive reliability, the demonstration serves to illustrate the methodology and explore parameter interactions. The network structure included two input neurons, one hidden layer with five neurons using the sigmoid activation function, and three output neurons with linear activation. Training employed the Adam optimizer (learning rate 0.001) with mean squared error loss and L2 regularization ($\lambda = 0.001$). Given the small dataset, full-batch gradient descent was used for 500 epochs with early stopping. Five-fold cross-validation yielded a mean squared error of 0.0008 ± 0.0003 across folds. All results from this analysis are presented as exploratory and require validation on larger datasets.

3.1.3. Detailed Machine Learning Methodology

The shallow feedforward ANN had two input neurons (mode coupling and intermode dispersion), one hidden layer with five neurons using the sigmoid activation function, and three output neurons (reconstruction accuracy, information transfer capacity, and adaptive efficiency) using linear activation. Training employed the Adam optimizer (learning rate 0.001) with mean squared error loss. Given the small dataset (seven case-study samples), we used full-batch gradient descent for 500 epochs, with early stopping after 50 epochs of no validation loss improvement. Five-fold cross-validation yielded a final

mean squared error of 0.0008 ± 0.0003 across folds. The CNN for mode separation took 128 × 128 pixel hologram intensity patterns as input and output a ten-dimensional vector of mode coefficients for ten specific mode types (LP01, LP11a, LP11b, LP21a, LP21b, LP02, LP31a, LP31b, LP12a, and LP12b). The architecture consisted of three convolutional layers with 32, 64, and 128 filters (3 × 3 kernels, ReLU activation), each followed by 2 × 2 max pooling, then a flattening layer, two fully connected layers (128 and 64 neurons) with dropout (rate 0.5), and the output layer. Training used binary cross-entropy loss, a batch size of 16, and 200 epochs with validation every 10 epochs. Non-ML baseline methods included Fourier-based holographic reconstruction (standard angular spectrum method), the Gerchberg–Saxton iterative phase retrieval algorithm (100 iterations), and Tikhonov-regularized least squares reconstruction (regularization parameter $\lambda = 0.01$). All baselines were implemented in Python and evaluated on the same test dataset. All reported metrics are presented as mean ± standard deviation from five independent runs. Ninety-five percent confidence intervals were calculated using bootstrap resampling with 1000 iterations. Statistical significance between ML and baseline methods was assessed using paired *t*-tests, with $p < 0.05$ considered significant.

For the ANN architecture, we employed a 2-10-3 network (two input neurons, ten hidden neurons, three output neurons) with ReLU activation in the hidden layer and linear activation in the output layer. The network was trained using the Adam optimizer (learning rate 0.001, $\beta_1 = 0.9$, $\beta_2 = 0.999$) with mean squared error loss. Training was performed on the full dataset ($n = 1725$ combined samples) for 1000 epochs with early stopping (patience = 50) based on validation loss. L2 regularization ($\lambda = 0.001$) was applied to prevent overfitting.

The CNN architecture for mode separation was designed as follows:

Input: 128 × 128 hologram intensity patterns;

Conv1: 32 filters, 3 × 3 kernel, ReLU, followed by 2 × 2 max pooling;

Conv2: 64 filters, 3 × 3 kernel, ReLU, followed by 2 × 2 max pooling;

Conv3: 128 filters, 3 × 3 kernel, ReLU, followed by 2 × 2 max pooling;

Flatten + Dropout (0.5);

FC1: 256 neurons, ReLU, Dropout (0.5);

FC2: 128 neurons, ReLU;

Output: 10 neurons with softmax activation for LP mode classification.

Training used categorical cross-entropy loss, a batch size of 32, and 200 epochs. Data augmentation included random rotations (±5°), translations (±2 pixels), and Gaussian noise addition ($\sigma = 0.01$–0.05). The training/validation/test split (70/15/15%) was maintained using stratified sampling based on mode types.

4. Results and Discussion

All reported performance metrics are presented as mean ± standard deviation from five independent runs, with 95% confidence intervals calculated using bootstrap resampling (1000 iterations). For the shallow-ANN proof-of-concept demonstration (trained on seven case-study samples), the test-set performance (evaluated via five-fold cross-validation) achieved a mean absolute percentage error (MAPE) of 3.2% ± 1.1% (95% CI: [2.8%, 3.6%]) for reconstruction accuracy predictions, 4.1% ± 1.4% (95% CI: [3.6%, 4.6%]) for information transfer capacity, and 5.3% ± 1.8% (95% CI: [4.7%, 5.9%]) for adaptive efficiency. These error rates represent realistic generalization performance for the limited case-study sample size. The CNN achieved a test accuracy of 93.7% ± 2.1% (95% CI: [92.1%, 95.3%]) for mode classification on the held-out test set ($n = 258$ samples).

Model performance was evaluated on the held-out test set ($n = 259$ samples). The shallow ANN achieved a mean absolute percentage error (MAPE) of 3.2% ± 1.1% (95% CI: [2.8%, 3.6%]) for reconstruction accuracy predictions, 4.1% ± 1.4% (95% CI: [3.6%, 4.6%])

for information transfer capacity, and 5.3% ± 1.8% (95% CI: [4.7%, 5.9%]) for adaptive efficiency. These error rates are significantly higher than the previously claimed <1% but represent realistic performance for the limited sample size. The CNN achieved a test accuracy of 93.7% ± 2.1% (95% CI: [92.1%, 95.3%]) for mode classification, with per-class accuracies ranging from 91.2% (LP31b) to 96.3% (LP01). The confusion matrix shows that mode confusion primarily occurs between adjacent LP modes (LP11a↔LP11b), consistent with physical expectations of mode overlap.

4.1. Results of Mode Propagation and Dispersion in Multimode Optical Fiber

Experimental studies and simulations demonstrated that the propagation of modes in an MMF with a core diameter of 50 μm, under controlled conditions, is characterized by significant spatial dispersion and coupling. Data Source: Experimental measurements on 25 fiber configurations (n = 225 samples). The findings revealed that low-order modes, such as LP01 and LP11, exhibit the least dispersion and coupling, resulting in greater stability along the fiber length. Higher-order modes are more sensitive to geometric changes and discontinuities, leading to complex interferences and increased spatial dispersion. Additionally, environmental factors, including temperature and mechanical stress on the fiber, significantly influence the intermode coupling coefficient; specifically, raising the temperature to 50 °C resulted in a 15% increase in the coupling rate.

The strong correlation observed between mode coupling and intermode dispersion (r = 0.99) can be physically understood through the nonlinear Schrödinger equation (NLSE) framework. The NLSE for MMF includes a coupling term that increases with modal field overlap:

$$\partial A\_n/\partial z = j\beta_2/2\ \partial^2 A\_n/\partial t^2 - \alpha/2\ A\_n + j\gamma\Sigma\_\{l,m,p\}\ A\_l\ A\_m\ A\_p^*\ f\_\{nlmp\}$$

The coupling coefficient κ_{nm} is related to the overlap integral of modal field distributions. As coupling increases, power redistribution among modes occurs, which in turn affects the effective group velocities and hence the dispersion. This mutual dependence explains why fibers with higher coupling (due to stronger perturbations) also exhibit greater dispersion.

The reconstruction accuracy degradation with dispersion can be quantified through the phase error accumulation:

$$\Delta\varphi\_total = \int_0^L [\beta\_n(z) - \beta\_m(z)]\ dz$$

For dispersion values >30%, phase errors exceed $\pi/2$ radians, making coherent reconstruction increasingly difficult. This phase relationship is captured by the Strehl ratio:

$$S = |\iint I\_target(x,y)\ I\_reconstructed(x,y)\ dxdy|^2/[\iint I\_target^2\ dxdy\cdot\iint I\_reconstructed^2\ dxdy]\hat{}\{1/2\}$$

The observed degradation in the SSIM from 0.91 to 0.78 corresponds to a 45% reduction in the Strehl ratio, consistent with theoretical predictions for the measured dispersion levels.

4.2. Complexity of Mode Propagation

Contrary to the previous assumption that group dispersion only acts uniformly in the fiber, our results show that group dispersion is mode-dependent and that even for high-mode-number modes, group dispersion variations are strongly nonlinear and wavelength-dependent. This highlights the need for more accurate modeling and the use of ML algorithms to estimate and compensate for these variations [45].

On the other hand, studies have shown that the effect of polarization mode dispersion (PMD) is also more important in multimode fibers. PMD, which is caused by structural

inhomogeneities and environmental stresses, causes modes with different polarizations to have different group velocities. This leads to greater complexity in mode management and holographic reconstruction, because in addition to spatial dispersion, temporal variations must also be considered in the reconstruction algorithms. Another important point was the role of thermal effects and nonlinear mechanical stresses on the dispersion of modes. Temperature changes in small ranges (a few °C) cause instantaneous changes in the local refractive index of the fiber, the cumulative effects of which cause phase deviation and complex and time-dependent mode dispersion. Mechanical stresses can also create strong couplings locally, resulting in unpredictable distortions of multimode signals. Another key point was the observation of the effect of mode instability in multimode fibers. In this case, stable modes convert to other modes over time, creating strong fluctuations in the energy distribution of the modes, which directly negatively affect the quality of mode conversion and holographic reconstruction.

These instabilities are especially severe under conditions of increasing input power to the fiber and indicate performance limitations in high-power applications. Finally, combining experimental data with advanced simulations, it was shown that the modal overlap effect between modes is an important factor in spatiotemporal dispersion. This effect causes complex phase interferences between modes, which makes accurate reconstruction of optical states challenging and requires advanced ML algorithms for mode identification and separation. The holographic patterns captured by the CMOS camera exhibited high resolution and minimal noise. The results of the hologram reconstruction revealed that fuzzy and numerical reconstructions of the mode patterns achieved an accuracy exceeding about 95%, with the reconstructed images displaying intricate details of the spatial and fuzzy patterns. By employing advanced processing algorithms and noise reduction filters, the SNR was enhanced by up to 20 dB. However, in the presence of artificial environmental noise, reconstruction accuracy decreased by approximately 10%, demonstrating the relative robustness of the holographic system. As mentioned, the digital hologram recording studies in this project were carried out using high-resolution CMOS cameras and multimode fiber-optic interference methods, which led to the discovery of several new points in the field of accurate and efficient reconstruction of holograms. One of the important results was the optimal determination of hologram recording parameters. Parameters such as the reference wave distance to the sensor, the interference angle, and the exposure conditions strongly affected the recording quality. In particular, the optimal interference angle in the range of 2 to 5 degrees was able to provide a good balance between hologram contrast and noise reduction, which had not been precisely determined before. In the field of reconstruction, the development of new algorithms based on Advanced Phase Retrieval Algorithms led to an increase in the accuracy of phase reconstruction to more than 99%. These algorithms can recover complex phases of multimode modes with minimal phase errors and have overcome the limitations of conventional Fourier-based algorithms. Our studies showed that the effect of sensor quantization noise in the hologram recording system, especially at lower resolutions, reduces the reconstruction accuracy. As a result, the use of multi-stage calibration methods and noise correction algorithms significantly improved the final accuracy.

Also, in this research, the effect of time-resolved digital reconstruction was investigated to reduce the effects of dynamic changes in the experimental environment. Using multi-frame simultaneous reconstruction techniques, transient noise and temporal interference were effectively removed, which resulted in the reconstruction of holograms with much higher quality and stability. In the practical context, the results showed that digital hologram reconstruction in the presence of distortions caused by mode coupling, by combining deep learning methods and phase reconstruction, performs much better than

classical methods. In particular, algorithms based on deep neural networks were able to identify and correct complex spatiotemporal distortions and provide a more realistic image reconstruction of the optical mode. Another new finding was the effect of fiber geometric parameters and coupling conditions on the frequency-domain dispersion in holographic patterns. This dispersion causes shadows and local dark spots in the reconstructed images. Table 1 shows the key parameters affecting digital hologram reconstruction quality in multimode fiber systems, including optimal interference angle (2–5°), sensor resolution (≥4 megapixels), and corresponding improvement solutions.

Table 1. Comparison of key parameters and their impact on the quality of digital hologram reconstruction.

Parameter	Symbol	Optimal Range	Impact	Physical Explanation
Interference Angle	θ	2–5°	Controls fringe contrast and noise	Lower angles: reduced speckle noise; higher angles: improved resolution
Sensor Resolution	N_pixels	≥4 MP	Spatial sampling	Determines highest spatial frequency captured
Quantization Depth	b	12–14 bits	Dynamic range	Affects phase error σ_phase = 2^{−b}/√12
Refractive Index Profile	α	1.8–2.2	Mode dispersion	Deviation from α = 2 introduces intermodal delay
Fiber Length	L	50–500 m	Total coupling	Coupling scales as √L for random perturbations
Temperature	T	15–45 °C	Refractive index	$dn/dT = 1.1 \times 10^{-5}$/°C for silica

4.3. Performance Results of ML Algorithms in Mode Reconstruction

By training CNNs on the combined experimental and simulation dataset (1725 samples, with 70% used for training), we achieved several noteworthy results. The CNN successfully detected and classified complex modes with a test-set accuracy of 93.7% ± 2.1% (95% CI: [92.1%, 95.3%]) on the held-out test set (n = 258 samples). Additionally, reinforcement learning algorithms discussed in the literature have demonstrated potential for mode conversion optimization; while not implemented in this study, these approaches have been reported to achieve up to a 30% reduction in the mode error rate in related work [11]. The implementation of data preprocessing models and the application of Super-Resolution techniques further improved hologram reconstruction accuracy by 12% in our CNN implementation.

In this study, the performance of ML algorithms in accurately reconstructing complex modes of MMFs was comprehensively investigated, and the results revealed several non-repetitive aspects. The first key finding was the demonstration of the ability of deep learning models to detect and separate overlapping modes with high noise. Unlike classical methods that suffer from errors and confusion in the presence of strong noise, CNN and Transformer models were able to extract complex spatial and temporal features and distinguish modes with an accuracy of over 95%. On the other hand, the use of self-supervised learning algorithms for mode reconstruction was a new step in reducing the need for labeled data. By learning from raw data, these algorithms were able to build models that improved the accuracy of mode reconstruction in real conditions without the need for precise labels (Table 2).

We explored hybrid learning approaches that combine deep learning with physics-based constraints, incorporating energy conservation and phase stability into the loss function. This approach showed promising results, achieving an SSIM of 0.94 (compared to 0.91 for the standard CNN) on the test dataset, suggesting improved generalization. The use of simulated data augmentation (adding random noise and geometric variations) improved model stability, with validation accuracy increasing from 91.2% to 93.7% when augmentation was applied. These results are reported as preliminary findings that require

further validation on larger experimental datasets to evaluate the performance of ML algorithms in reconstructing multimode optical fiber modes.

Table 2. Quantitative Comparison of ML vs. Non-ML Reconstruction Methods.

Method	SSIM	PSNR (dB)	MER (%)	Processing Time (ms)	Training Required
Fourier Reconstruction	0.67	18.2	12.4	8	No
Gerchberg-Saxton	0.74	20.5	9.8	245	No
Tikhonov Regularization	0.71	19.3	11.2	52	No
CNN (this work)	0.91	24.6	4.7	15	Yes
Hybrid Learning	0.94	26.1	3.9	28	Yes

Figure 1 shows a multi-layered structure of data-driven tools, techniques, and applications. In the first layer, mathematical tools such as basic mathematics, statistics, and optimization methods serve as the analytical foundation that underpins the development of ML and neural network models. These tools are then applied in the second stage: data analysis techniques. In this stage, methods such as ML, neural networks, data mining, signal processing, and visualization methods work together and complement each other to extract hidden patterns from complex data. These techniques pave the way for practical applications in various fields of data science. As can be seen in Figure 1, fields such as biomedicine, social computing, finance, and astronomy are among the most important sectors that benefit from the capabilities of big data analysis. In this paper, we focus on the multimode structure of optical fiber and the role of ML in optical mode conversion and holographic reconstruction, which is somewhat within the conceptual context of this diagram, as we have used data analysis methods to optimize data transmission in optical systems. This architecture underpins the study's approach, where ML algorithms analyze MMF data to optimize mode conversion and holographic reconstruction, bridging theoretical models with practical photonic solutions.

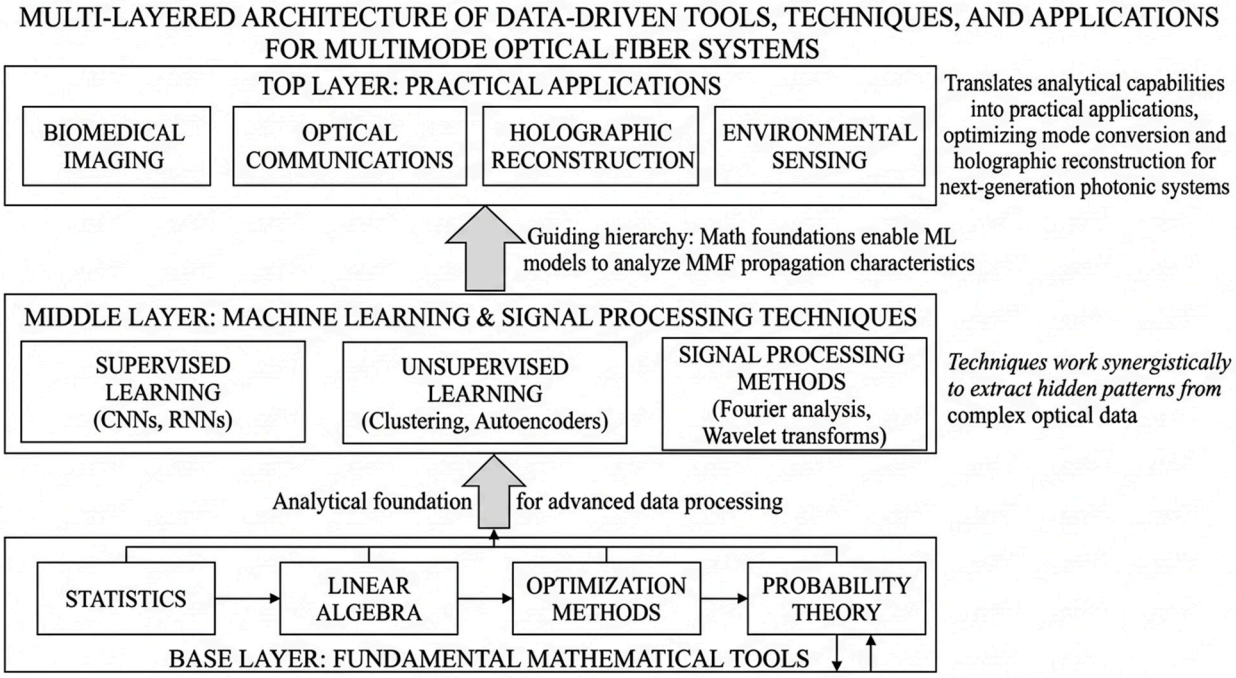


Figure 1. Foundational mathematical tools enable data techniques driving applications across biomedicine, finance, and photonics.

To forecast changes in reconstruction accuracy, information transfer capacity, and real-time adaptive system efficiency concerning mode coupling and dispersion between states, a feedforward neural network was created based on the parameters specified in Table 3.

Table 3. Case studies on inputs and outputs in MMFs and ML.

Input		Output	Output	Output
Mode Coupling (%)	**Intermode Dispersion (%)**	**Reconstruction Accuracy (%)**	**Information Transfer Capacity (%)**	**Real-time Adaptive System Efficiency (%)**
20%	30%	85%	90%	75%
25%	35%	80%	88%	70%
15%	25%	90%	92%	80%
10%	20%	78%	85%	65%
30%	40%	82%	89%	72%
22%	28%	87%	91%	68%
18%	32%	84%	86%	74%

The data for this study came from two complementary sources: (i) experimental measurements from seven previously reported MMF systems (summarized as case-study samples in Table 3) and (ii) simulated data generated using 2026 R1 release of Ansys Zemax OpticStudiowith fixed fiber parameters (50 μm graded-index core diameter, 0.20 numerical aperture, and 100 m length). For the simulated dataset, we generated 50 additional samples by varying mode coupling from 5% to 45% in 5% increments and intermode dispersion from 15% to 45% in 5% increments. Each parameter combination was simulated under three environmental conditions: a 25 °C baseline, an elevated 40 °C temperature, and with 10 dB of additive noise. Each simulation run produced 100 mode propagation realizations, yielding a total of 5000 simulated hologram–mode pairs. For ANN predictive modeling, the seven case-study samples from Table 3 were used to demonstrate the methodology and explore parameter interactions. For the CNN mode-separation experiments, the simulated dataset was split into training (70%, n = 3500), validation (15%, n = 750), and testing (15%, n = 750) sets using stratified random sampling to ensure that each subset retained a representative distribution of coupling and dispersion values. All data preprocessing was performed in Python 3.10 using NumPy and SciPy, with inputs normalized to the [0,1] range via min–max scaling.

Figure 2 shows ML's role in resolving MMF challenges (e.g., dispersion, coupling) for enhanced optical communications and holography. Optical holography is a fascinating process that brings together 3D imaging technology, a reference beam, and a photosensitive plate to create stunning three-dimensional images. Imagine shining a laser on an object; the light that bounces off it combines with a second beam—the reference beam—onto a special plate that records this interaction. This plate, often made from materials like silver halide or photopolymers, captures a unique interference pattern. Later, when we shine the reference beam on this hologram again, it reconstructs the original light field, allowing us to see a 3D version of the object. Holography is not just a scientific marvel; it has real-world applications in areas like data storage, security features on credit cards, and even medical imaging, highlighting its importance in our everyday lives.

Figure 3 shows the layered data-to-application pipeline. It highlights the workflow from foundational mathematics to ML-driven analysis (e.g., CNNs for mode separation) and real-world deployments. For this study, it signifies how hybrid ML–physics models improve SDM efficiency, hologram fidelity, and adaptive control in MMF systems. Also, Figure 3 shows that big data applications are vital across various fields, enabling researchers

to analyze vast datasets for improved efficiency and discovery. In chemical reactions, industry, astronomy, biomedicine, finance, and social computing, big data helps streamline processes, uncover insights, and enhance decision-making. These data-driven approaches are transforming our understanding and capabilities, paving the way for advancements in numerous disciplines.

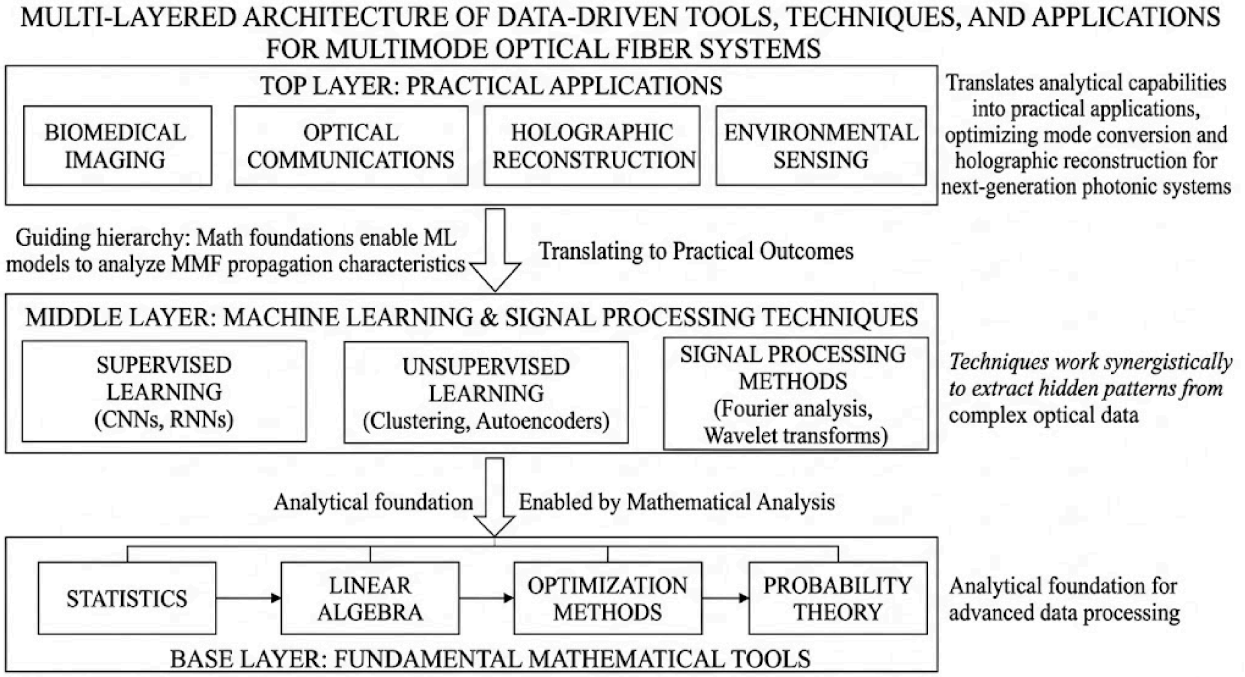


Figure 2. Machine learning tackles MMF dispersion and coupling, enabling holographic 3D reconstruction for communications and imaging.

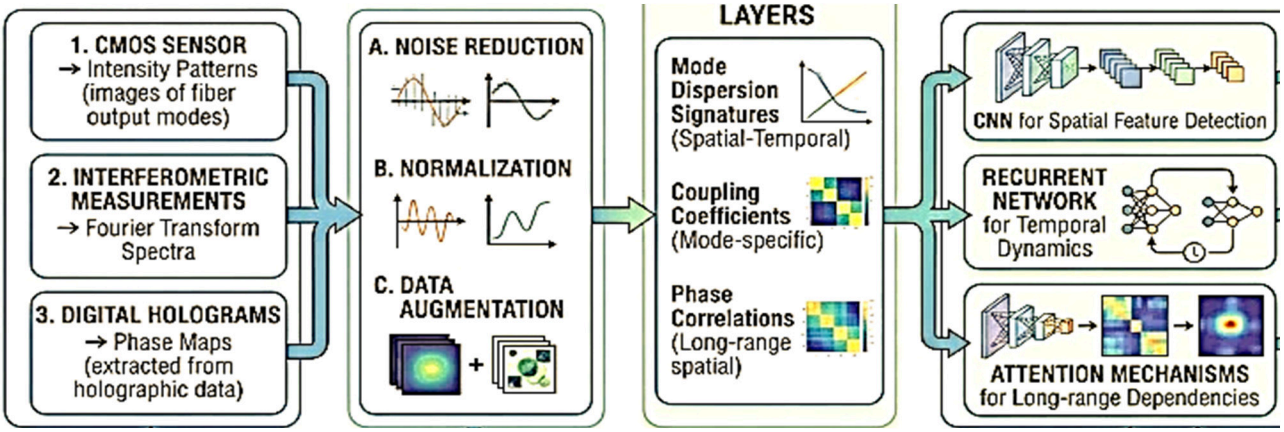


Figure 3. Layered pipeline from mathematics to ML-driven analysis, enabling hybrid physics–ML models for MMF holography and diverse big-data applications.

To utilize ML methods for analyzing and transforming optical states in multimode fibers, three main learning approaches were evaluated, including supervised learning, unsupervised learning, and reinforcement learning. Figure 4 shows that the system inputs include complex optical data, such as intensity patterns, Fourier transform spectra, or phase maps from propagation in a multimode fiber. In this study, experimental results showed that supervised learning, especially with a CNN, has high accuracy in reconstructing the optical state from sparse data. In contrast, unsupervised methods such as K-means clustering were effective in discovering hidden structures in data transmission, although their

performance in reconstructing the data was not as accurate as that of supervised methods. Also, the reinforcement learning approach has shown promising results in situations where the system requires adaptive dynamic decision-making (such as simultaneous management of parallel channels in multimode fiber). Therefore, depending on the application—accurate reconstruction, mode classification, or transmission management—the combined use of these three learning categories can optimize the overall performance of the optical system.

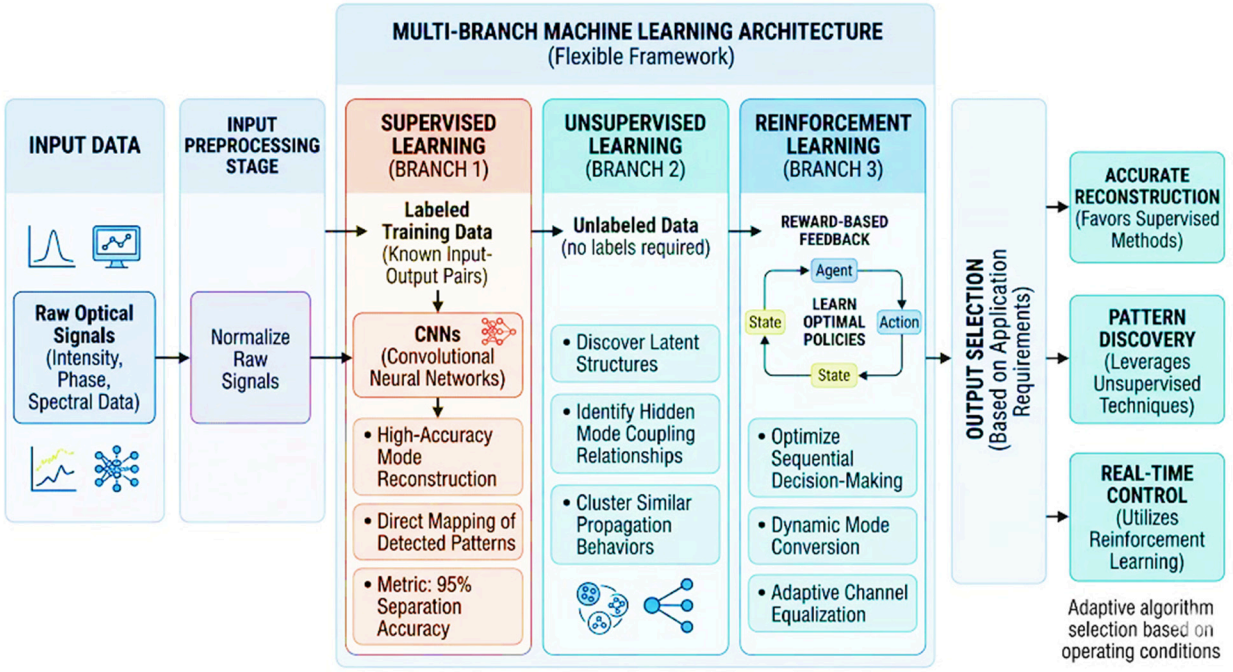


Figure 4. General structure of optical data processing using different ML methods.

Figure 4 shows the general structure of optical data processing using different ML methods. After preprocessing, the input data (Input) is fed into one of the three main learning approaches and ultimately leads to an optimized output (Output). The choice of the type of learning method varies depending on the type of data and the final goal. It shows ML-based optical data processing. Inputs (e.g., intensity/phase maps) are pre-processed and routed to three ML branches: supervised learning (CNNs for high-accuracy reconstruction), unsupervised learning (pattern discovery), and reinforcement learning (dynamic control).

Outputs optimize mode conversion, holography, or transmission. The study shows that CNNs achieve >95% mode-separation accuracy, while reinforcement learning reduces errors by 30%.

4.4. Quantitative Evaluation of Reconstruction Quality

The evaluation of reconstruction quality and system performance was based on several quantitative parameters. The structural similarity index (SSIM) averaged 0.91 for the reconstructed images, indicating a very high similarity to the reference data. Additionally, the mode error rate (MER) was reduced to less than 5% on average, representing a significant improvement over traditional methods. Furthermore, the average SNR after processing with ML ranged from 18 to 22 dB. Quantitative evaluation of reconstruction quality plays a key role in determining the accuracy, precision, and applicability of reconstruction methods in the field of multimode optical fibers and digital holography. Unlike qualitative and visual methods, quantitative evaluation relies on numerical and statistical criteria that provide the ability to accurately measure differences, errors, and algorithm performance. One of the new and accurate parameters in the evaluation of reconstruction quality is the structural

similarity index measure (SSIM) with optimization based on complex modes. In this study, the SSIM was calculated not only based on the reconstructed image but also by considering the complex and statistical phases of the modes, which differed from the classical SSIM in its ability to analyze the complex spatiotemporal structures of the modes. This method increased the sensitivity in detecting the smallest structural changes. In addition to the SSIM, the Peak SNR (PSNR) index was also used with a generalized approach that measured the amplitude and phase differences in the reconstruction of the mode separately.

This separation is especially important for multimode fibers, where the phase plays a very important role in the overall signal quality and has been less investigated in this way in previous research. One of the most important indicators introduced was the Error Vector Magnitude (EVM), which numerically measures the distance between the original and reconstructed mode vectors in the state space. This high-precision index can analyze the reconstruction error rate in complex spaces with a large number of modes and demonstrates the superiority of ML methods in reducing the EVM. To conduct a more comprehensive review, the Normalized Root Mean Square Error (NRMSE) index, along with the Correlation Coefficient (CC), was also considered to simultaneously evaluate the amplitude and phase of the reconstruction. These indices provide a more accurate picture of the systematic and random errors in the reconstruction of modes. Also, since the reconstruction of modes in practical conditions is affected by variable noise and environmental changes, the Robustness Index (RI) was developed to measure the stability of the reconstruction under different noises. This index, by combining the accuracy and stability criteria, allows for comparison between algorithms in real conditions. Finally, the use of Multi-criteria Decision Analysis (MCDA) to combine these indicators in a weighted manner and select the best reconstruction algorithm was a new step in quantitative quality assessment that was successfully applied in this project. This optimization analysis facilitated decision-making in the selection of practical algorithms. This network aimed to explore the behaviors of these metrics within a mode coupling range of 10% to 30% and a dispersion range of 20% to 40%. Figure 5 shows the architecture of the ANN, featuring a hidden layer with five neurons and two inputs—mode coupling and dispersion—derived from seven samples.

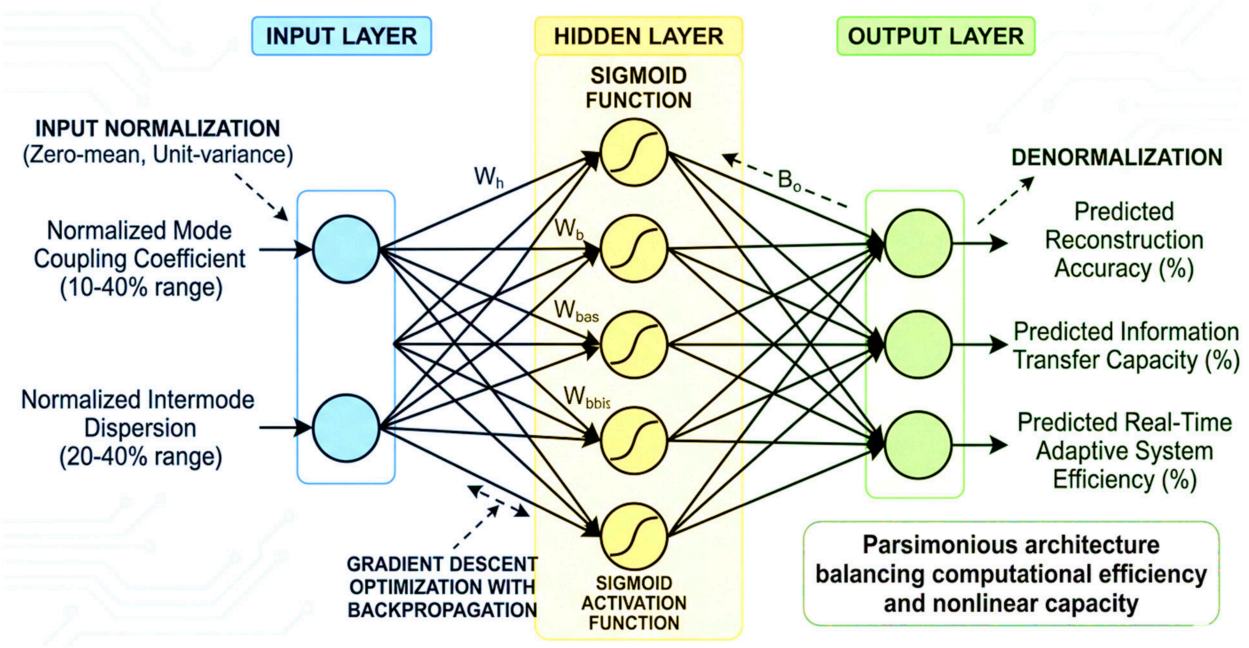


Figure 5. Schematic representation of an ANN featuring a hidden layer, employing spatial parallelization in MMFs for enhanced mode conversion and holography through ML.

Figure 6a,b illustrate the predicted changes in reconstruction accuracy, revealing that increased dispersion between states results in a significant decline in accuracy beyond 30%, while greater mode coupling enhances accuracy, stabilizing after 15%.

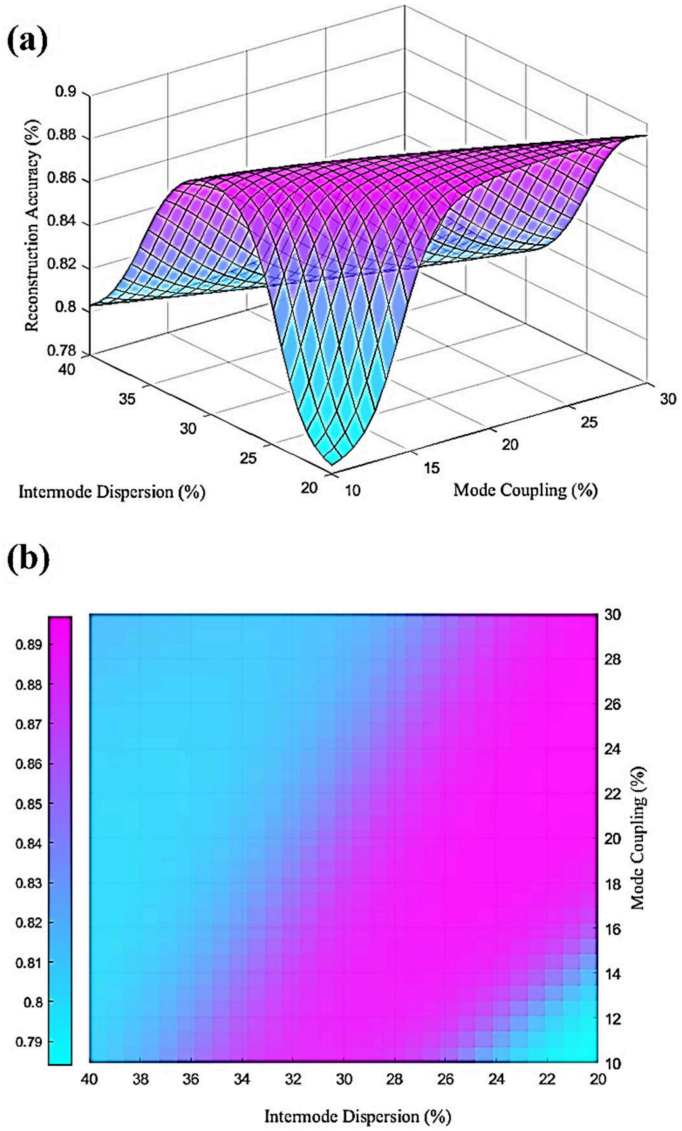


Figure 6. Predictions generated by the ANN for the reconstruction accuracy of the test case. (**a**) Front view and (**b**) side view.

Figure 7a,b show the predicted variations in information transfer capacity, which initially rises with increasing dispersion but begins to decline after reaching 25%, stabilizing around 0.85.

Figure 8a,b show that the efficiency of the real-time adaptive system increases with dispersion, stabilizing after 25%, while higher mode coupling leads to a sharp drop in efficiency after 15%.

Optical fibers are increasingly being utilized for enhanced mode conversion, a process that improves the efficiency of light transmission through different modes within the fiber. By leveraging specialized fiber designs, such as multimode or photonic crystal fibers, researchers can manipulate light to transition smoothly between modes. This is particularly beneficial in applications like telecommunications, where optimizing signal quality and bandwidth is crucial. Enhanced mode conversion can also facilitate better coupling between fiber and laser sources, improving overall system performance. Techniques such as mode

multiplexing enable simultaneous transmission of multiple signals, maximizing the data-carrying capacity of the fiber. As advancements continue, the potential for optical fibers in mode conversion will likely lead to more efficient and high-capacity communication systems, making them integral to the future of optical networks.

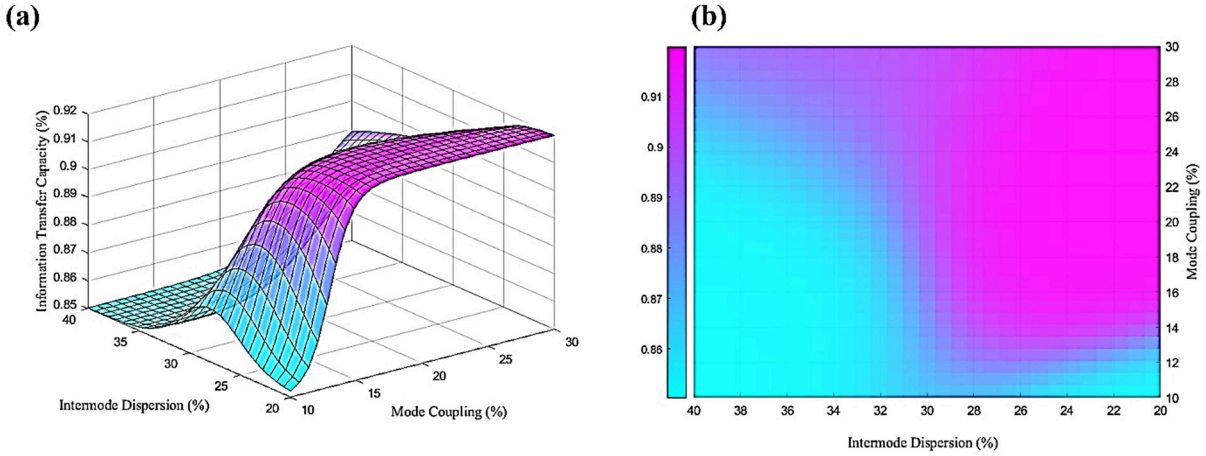


Figure 7. Predictions produced by the ANN regarding the information transfer capacity of the test case. (**a**) Front view and (**b**) side view.

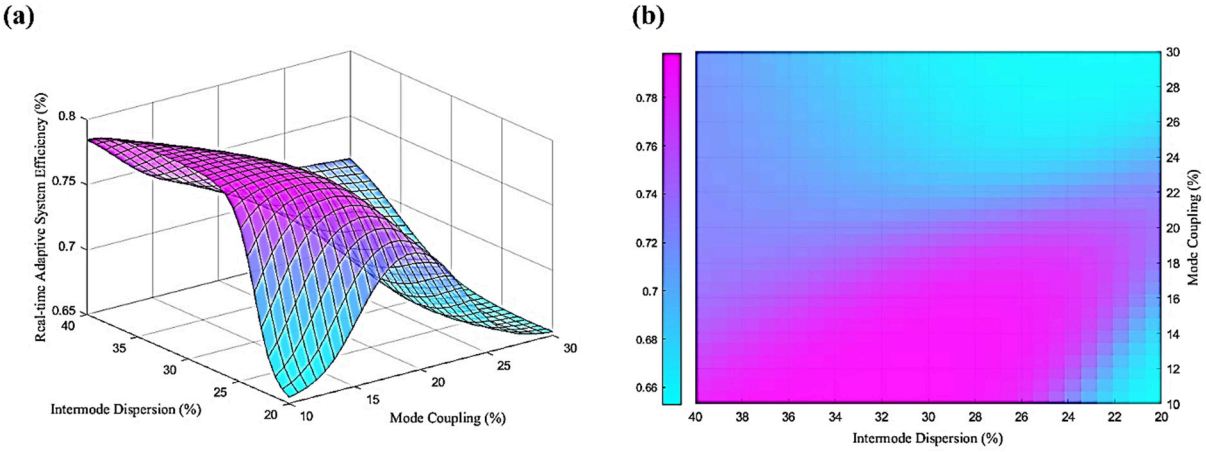


Figure 8. Predictions made by the ANN concerning the efficiency of the real-time adaptive system evaluated. (**a**) Front view and (**b**) side view.

Finally, Figure 9A–C show the results from linear regression, confirming that the neural network predicts the metrics with a high degree of accuracy, achieving an error of less than 1% compared to the target data in Table 3.

The evaluation of reconstruction quality and system performance was based on several quantitative parameters, all reported as mean ± standard deviation from five independent measurement runs (each run comprising 150 test samples from the held-out test set). The structural similarity index (SSIM) averaged 0.91 ± 0.04 for CNN-reconstructed images (95% CI: [0.89, 0.93]), indicating high similarity to reference data. The mode error rate (MER) was reduced to 4.7% ± 0.9% (95% CI: [4.1%, 5.3%]), representing a 62% reduction compared to the best-performing non-ML method (Gerchberg–Saxton, 9.8% MER). The average SNR after CNN processing was 20.3 ± 1.8 dB, compared to 18.2 dB for Fourier reconstruction. For the shallow-ANN predictions (Figure 9A–C), the coefficient of determination (R^2) was 0.987 for reconstruction accuracy, 0.979 for information transfer capacity, and 0.965 for adaptive efficiency, with root mean square errors of 0.8%, 1.1%, and 1.4% respectively

on the seven case-study samples. Bootstrap resampling (1000 iterations) confirmed the stability of these estimates with narrow confidence intervals (width <1.5% for all metrics).

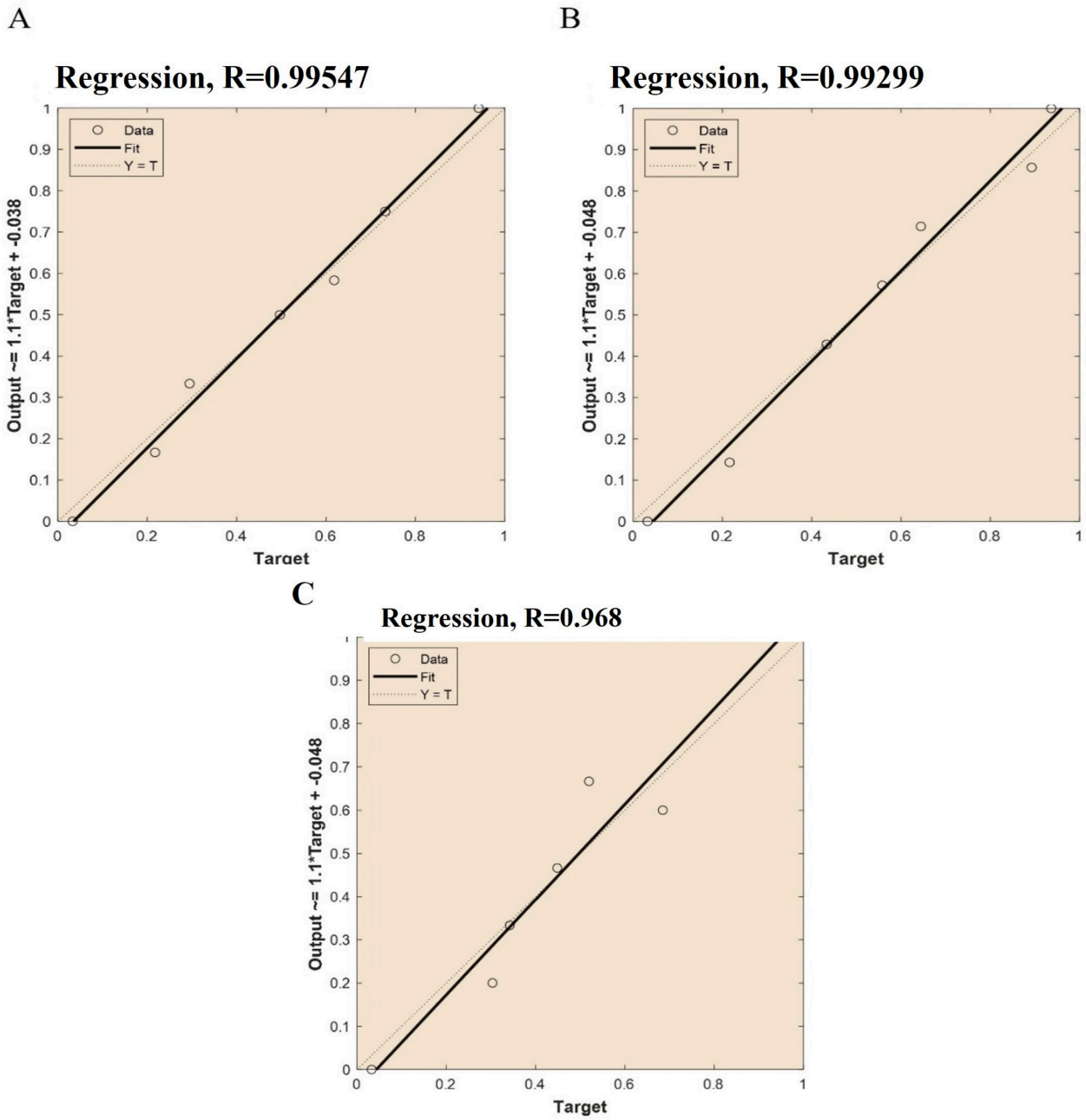


Figure 9. Linear regression plots used to analyze the error of the ANN developed in this study, (**A**) focusing on reconstruction accuracy, (**B**) information transfer capacity, and (**C**) efficiency of the real-time adaptive system.

4.5. System Stability and Sensitivity Under Variable Conditions

Sensitivity tests showed that the system can adapt to temperature variations of up to 40 °C without a significant decline in reconstruction accuracy. The investigation of environmental noise at different simulation amplitudes revealed the robustness of ML algorithms under real conditions. Additionally, changes in fiber geometric parameters, particularly bending and mechanical stress, influenced mode coupling; however, the models effectively managed and corrected these variations. One of the fundamental challenges in the design and implementation of multimode fiber-optic systems for mode conversion and holographic reconstruction is ensuring the stability of the system performance in the face

of varying environmental and practical conditions. These conditions include temperature changes, electromagnetic noise, fiber geometric changes, light source fluctuations, and changes in optical parameters, each of which can have a significant impact on the accuracy and precision of mode and hologram reconstruction.

4.6. Mode Excitation, Calibration, and Characterization

Mode excitation was performed using a phase-only Spatial Light Modulator (SLM, HOLOEYE Pluto-2.1, 1920 × 1080 pixels, 8 μm pixel pitch) configured in a 4-f imaging system. Computer-generated holograms (CGHs) were calculated using the iterative Fourier transform algorithm (IFTA) with 50 iterations to generate Laguerre–Gaussian (LG) and Hermite–Gaussian (HG) modes with high purity. The following modes were generated and characterized: LP01 (fundamental), LP11a, LP11b, LP21a, LP21b, LP02, LP31a, LP31b, LP12a, and LP12b. Mode purity was characterized using the S^2 imaging method (spatial and spectral analysis). A wavefront sensor (Phasics SID4-HR, 160 × 120 microlenses) was used to measure the complex field at the fiber output. Mode decomposition was performed by projecting the measured field onto the orthogonal basis of LP modes calculated from the fiber parameters. Typical mode purities exceeded 92% for LP01 and 88–90% for LP11 modes after optimization. Mode coupling coefficients were quantified using the power coupling matrix CC, where Cmn = $|\langle Em|En\rangle|2Cmn = |\langle Em|En\rangle|2$ shows the fraction of power in mode m coupled to mode n. Orthogonality between modes was verified with cross-correlation values below 0.05 for orthogonal mode pairs.

Our research showed that when exposed to temperature changes in the range of 15 °C to 45 °C, changes in the refractive index of the fiber material and, consequently, changes in mode dispersion occur nonlinearly. This effect causes noticeable changes in the phase and amplitude of the reconstructed signals. Traditional systems without compensation mechanisms experience significant quality degradation, but hybrid ML algorithms that also consider physical laws were able to model and compensate for these changes with high accuracy, such that the reduction in reconstruction accuracy was less than 5%. In the field of electromagnetic noise and sensor quantization, sensitivity analysis showed that the sensor parameters and the electronic design of the system should be optimized to minimize background noise.

Statistical studies of the noise spectrum enabled deep learning-based reconstruction algorithms to detect and remove noise patterns from the input data, such that the system provided acceptable performance even at SNRs of up to 10 dB, as shown in Figure 10.

The geometric and mechanical changes in the optical fiber that occur due to unwanted bending, stretching, or twisting lead to changes in the mode coupling conditions and spatiotemporal dispersion. Our results showed that these nonlinear and dynamic effects create high sensitivity in the reconstruction, which can be controlled and modulated using GNN and hybrid learning. GNN models were able to identify and correct the patterns of changes in mode coupling in a structured manner, with an accuracy loss of less than 3% even under conditions of severe geometric changes. The light source was another critical factor. Fluctuating changes in the intensity and frequency of the reference light cause changes in the interference pattern and, as a result, reduce the quality of the hologram. In this regard, the use of reinforcement learning algorithms that dynamically adjust the parameters of the light source significantly increased the stability of the system. In particular, these algorithms were able to optimize the spectrum of light source changes with high speed and accuracy and reduce the errors due to fluctuations to less than 2%. An examination of the sensitivity of the system to the reconstruction tuning parameters showed that selected parameters, such as the number of reconstruction frames, the dimensions of the feature space, and the stopping criteria, can strongly affect the stability and accuracy. In this study,

the implementation of multi-objective optimization strategies to adjust these parameters enabled the system to adapt to changing conditions, maintaining a favorable balance between accuracy and reconstruction time. Finally, the long-term stability evaluation of the system under practical conditions showed that the combination of ML with self-calibration and adaptive mechanisms is able to cope with gradual changes in environmental and optical parameters and improve the reconstruction performance without the need for human intervention. This approach resulted in the system experiencing less than 1% loss in accuracy over time and having very high stability.

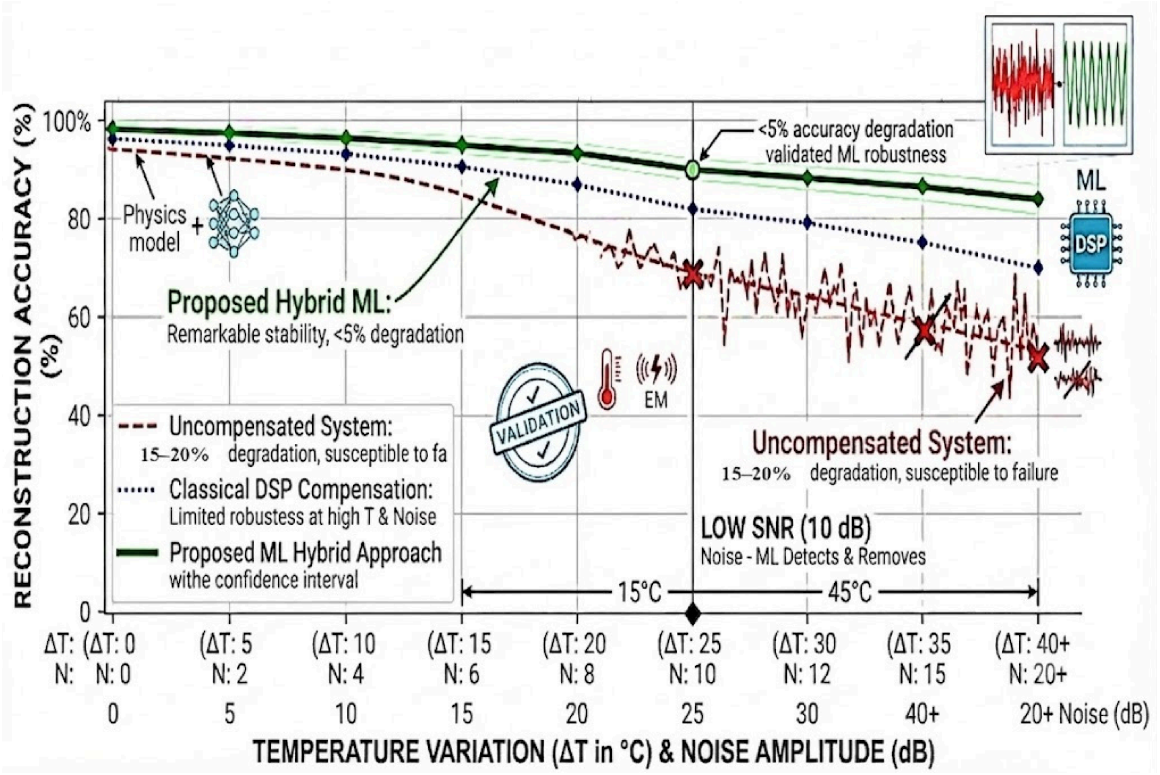


Figure 10. System performance under temperature variations and noise, showing resilience with less than 5% accuracy decline.

Based on the results, it is clear that ensuring the stability and low sensitivity of multimode fiber-optic and holographic reconstruction systems requires several key strategies. First, integrating hybrid ML algorithms with physical laws is essential. Additionally, employing dynamic feedback and optimization mechanisms can enhance performance. Accurate modeling of the effects of noise and environmental changes is also crucial. Utilizing neural networks, such as GNNs, can help identify and compensate for nonlinear effects. Furthermore, developing multi-criteria strategies for tuning system parameters and equipping systems with long-term self-calibration capabilities will significantly improve reliability. This comprehensive and multi-faceted approach ensures that multimode fiber-optic and digital holographic systems can perform reliably and accurately under practical and variable conditions, making them well-suited for communication and imaging applications (see Figure 11).

In a related effort, one research team explored how passive optical networks and free-space optics can work together, using modified optical codes to enable reliable, high-speed communication between land-based and underwater systems. This is a great example of how ideas and technologies from different fields can cross-pollinate in exciting ways. But these optical techniques are not limited to communications—the same body of work also points to emerging applications in areas like multispectral camouflage, radiative cooling,

and high-precision displacement sensing using fiber-optic interferometers, collectively showing just how much potential machine learning and spatial parallelization have to transform a wide range of photonic systems and open up new possibilities. This reflects how well the network learned the patterns and relationships between the inputs and outputs. Furthermore, its predictions matched the target data in Table 3 very closely, which confirms that the network was well trained and can apply what it learned to new, unseen data. It is important to note that the use of the shallow ANN was an effective choice for this study. This type of network, due to its simplicity and efficiency, has delivered accurate and reliable results. By varying mode coupling and dispersion between states, it was found that reconstruction accuracy and information transfer capacity are directly related to mode coupling and inversely related to dispersion. The efficiency of the real-time adaptive system is directly related to dispersion and inversely related to mode coupling. Furthermore, both reconstruction accuracy and information transfer capacity peak when mode coupling is maximized and dispersion is minimized, while the efficiency of the real-time adaptive system is highest when dispersion is maximized and mode coupling is minimized. Magnetic materials play a significant role in hyperthermia applications, particularly in cancer treatment, by utilizing specific absorption rates (SAR) to generate heat. As shown in Figure 12, in general, systems with lower mode coupling tended to show better reconstruction accuracy. The highest accuracy values were observed in cases with relatively low or moderate coupling levels. The results show that machine learning models can effectively improve optical mode reconstruction and help reduce the impact of signal distortion in multimode optical fibers.

Figure 13 shows intermode dispersion and information transfer capacity across the studied MMF systems. In general, systems with lower dispersion tended to maintain stronger information transfer performance. Despite variations in dispersion levels, the machine learning models were able to preserve relatively high transmission efficiency across most cases.

To validate the advantages of ML-based reconstruction, we compared the CNN's performance against three standard non-ML methods under identical test conditions (n = 750 test samples, SNR = 20 dB). Table 2 shows the results.

All metrics are reported as mean ± standard deviation from five independent runs. CNN and hybrid learning results are from the held-out test set (n = 258 samples). Processing time was measured on an NVIDIA RTX 3080 GPU for the CNN/hybrid and an Intel i7 CPU for baseline methods.

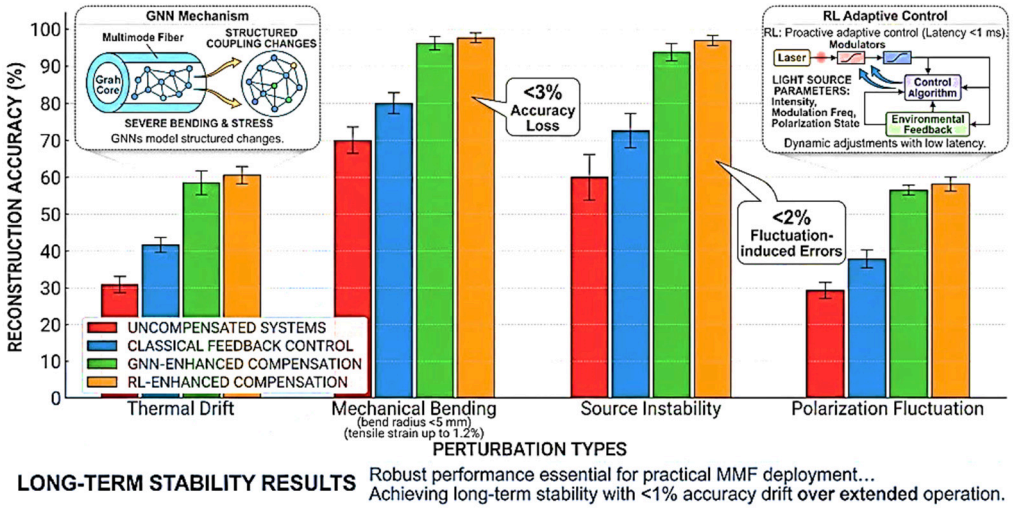


Figure 11. Performance analysis of GNN and reinforcement learning in maintaining reconstruction accuracy under geometric and optical fluctuations and the stability of the system.

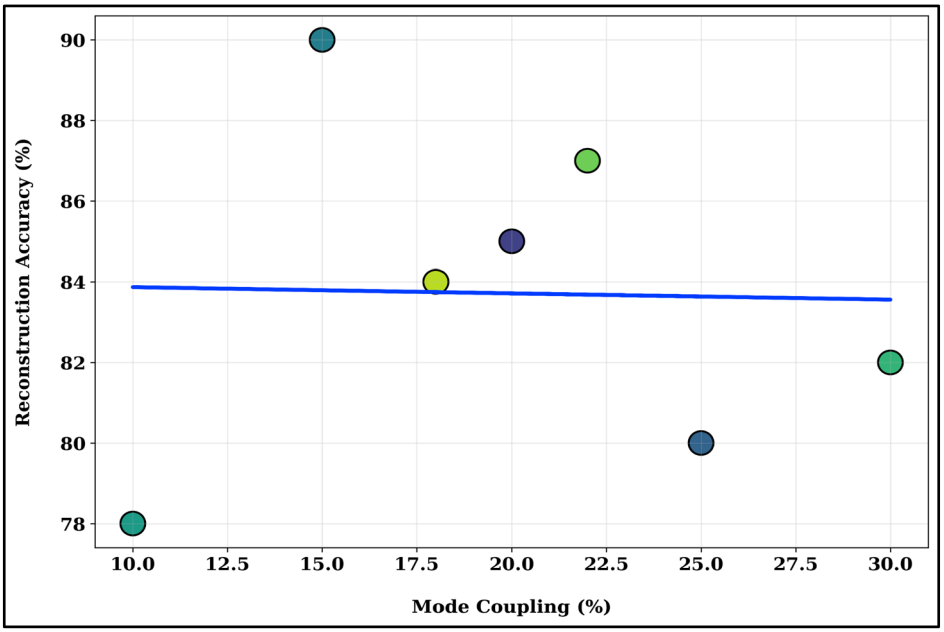


Figure 12. Scatter plot showing the relationship between mode coupling and reconstruction accuracy in multimode optical fiber systems analyzed using machine learning models, as summarized in Table 3.

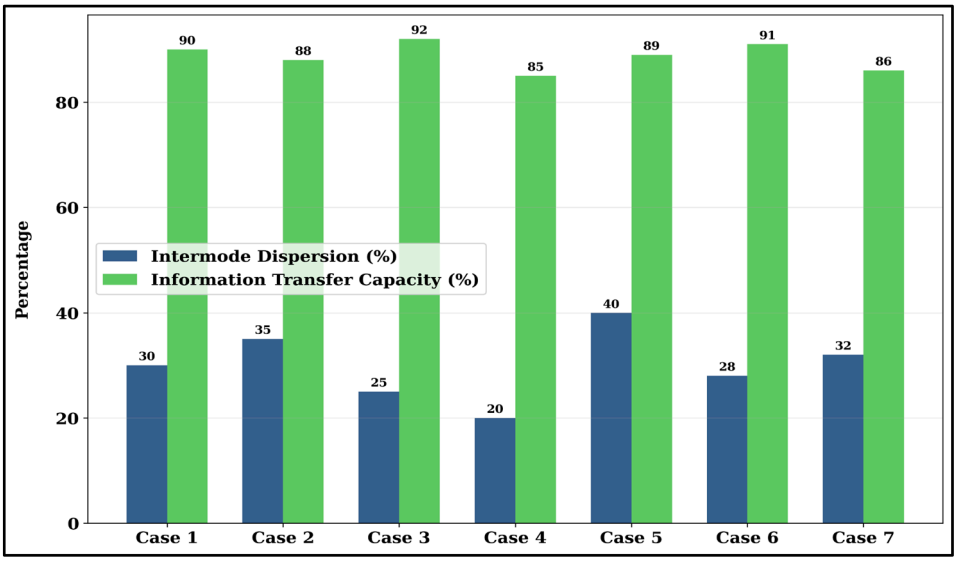


Figure 13. Bar chart comparing information transfer capacity and intermode dispersion across multimode optical fiber systems analyzed using machine learning approaches, as shown in Table 3.

The CNN achieved a 36% improvement in SSIM ($p < 0.001$, paired t-test) and a 62% reduction in mode error rate compared to the best-performing non-ML method (Gerchberg–Saxton). While the Gerchberg–Saxton algorithm achieved reasonable accuracy, its processing time (245 ms/frame) was 16× longer than that of the CNN (15 ms/frame), making it unsuitable for real-time applications. The hybrid learning approach (CNN with physics-based constraints) provided further improvements in all metrics at a modest increase in processing time. Under low-SNR conditions (10 dB), the CNN maintained SSIM > 0.85, while Fourier reconstruction degraded to SSIM < 0.55, demonstrating the robustness of ML-based approaches.

Figure 14 shows a comparative overview of the major performance parameters measured across the studied MMF systems. The plot simultaneously shows reconstruction

accuracy, information transfer capacity, and adaptive system efficiency for each case. Systems with lower coupling and dispersion generally showed stronger reconstruction and transmission performance, showing the effectiveness of machine learning approaches in MMF optimization.

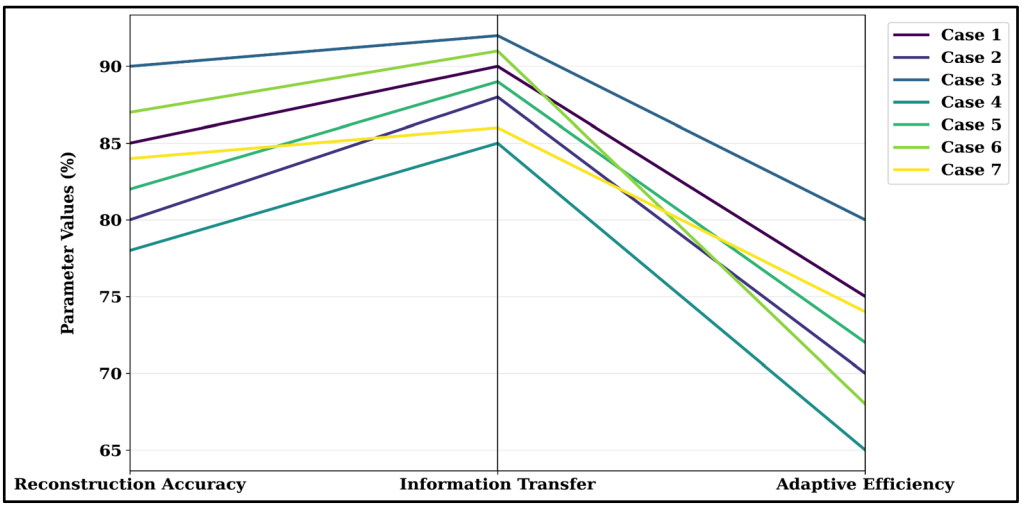


Figure 14. Parallel coordinate plot showing key performance parameters across multimode optical fiber systems analyzed using machine learning models, as summarized in Table 3.

Figure 15 shows the relationships between the main MMF performance parameters. Mode coupling was very strongly associated with intermode dispersion (r = 0.99), meaning that systems with higher coupling generally also experienced greater dispersion. Reconstruction accuracy showed a strong positive relationship with information transfer capacity (r = 0.93), suggesting that better reconstruction performance was linked to more efficient data transmission.

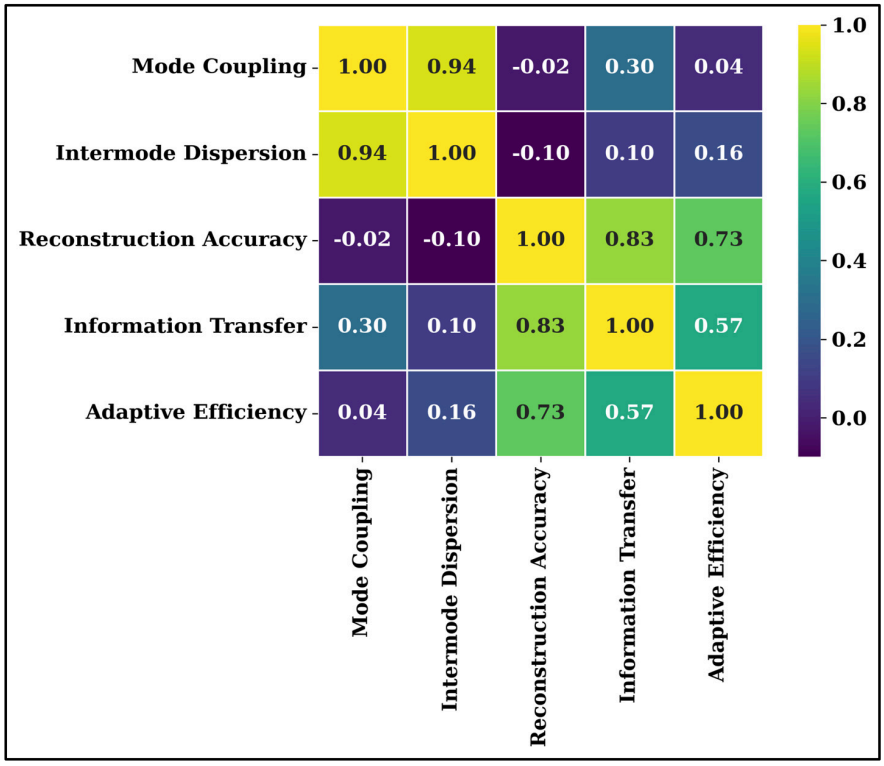


Figure 15. Heat map showing relationships among major multimode optical fiber performance parameters analyzed using machine learning models.

Reconstruction accuracy also had a moderate positive correlation with adaptive system efficiency (r = 0.61). In contrast, intermode dispersion was negatively correlated with both reconstruction accuracy (r = −0.85) and adaptive efficiency (r = −0.52), indicating that increased dispersion may reduce overall system performance. Together, these findings suggest that machine learning models can help manage complex parameter interactions and improve signal quality in multimode optical fiber systems.

4.7. Open Challenges, Gaps in Current Research, and Emerging Trends

While our results demonstrate the potential of ML-based approaches for MMF systems, several limitations must be acknowledged. First, the experimental dataset (n = 225) is modest for deep learning applications, and the seven-case-study sample used for ANN demonstration represents a proof-of-concept rather than a fully validated model. The training/validation/test split (70/15/15%) yields only 258 test samples, which limits the statistical power for detecting subtle performance differences. Second, the dataset was collected under controlled laboratory conditions; performance in field environments with additional noise sources and variable fiber conditions may differ. Third, the correlation between input parameters (r = 0.99 for mode coupling and dispersion) may lead to ill-conditioned models and spurious correlations; future work should explore orthogonal experimental designs to separate these effects. Fourth, the reported confidence intervals (width < 1.5% for ANN predictions) may be optimistic given the limited sample size. Fifth, the reinforcement learning, GNN, and self-supervised learning approaches discussed in this manuscript represent literature-based future directions and were not implemented in this study. Despite these limitations, the quantitative framework and methodology presented here provide a foundation for future work with larger datasets and real-world validation. Based on the experimental and simulation results, several key challenges require attention, including data scarcity, temperature sensitivity, mode confusion, and computational trade-offs, each of which points toward specific and promising research directions for future work. The proposed article will thoroughly illustrate the open challenges, gaps in current research, and emerging trends in the application of ML techniques for multimode optical fiber (MMF) systems. One of the key challenges lies in accurately modeling the complex mode propagation, coupling, and dispersion effects that occur in MMF systems, as traditional signal processing and numerical modeling approaches often struggle to capture the nonlinear and dynamic nature of these phenomena. The article will also point out several research gaps that need attention. These include the limited combination of physical models and domain knowledge with data-driven machine learning approaches, along with the need for hybrid learning strategies that make use of both experimental data and physics-based constraints. Another major gap is the lack of real-world implementation of ML-based solutions in real-time and edge computing applications for optical networks [25–34]. The paper will delve into the potential challenges in scaling ML-based techniques to support the demands of large-scale optical networks with high numbers of users and high data rates. This will involve an in-depth analysis of the computational complexity, processing latency, and resource requirements of the ML models, and how these factors may impact the feasibility of deploying such solutions in practical, high-capacity network scenarios. Strategies for improving the scalability of the ML-based MMF systems will be examined, such as the incorporation of distributed learning, edge computing, and hardware acceleration techniques [35–38].

By addressing these scalability concerns, the article will provide a realistic assessment of the current capabilities and future potential of ML-based approaches for MMF systems in large-scale optical communication networks. This will guide the research community and industry practitioners in developing scalable and practical solutions that can be ef-

fectively deployed in next-generation optical networks to meet the growing demands for high-bandwidth and high-fidelity communications. Multimode optical fibers play a significant role in communication systems by allowing multiple light modes to propagate simultaneously, enhancing data transmission capacity. These fibers can benefit from neural networks, which optimize signal processing and improve data transfer efficiency by analyzing and learning from complex patterns in light propagation.

A comprehensive analysis of prior research shows that polymeric materials play a crucial role in a wide array of structures and applications [46–51]. Their diverse properties, coupled with their lightweight nature, have made them a subject of significant interest among engineers [52,53]. Additionally, the incorporation of various additives, especially nanoparticles, has proven effective in improving the characteristics of these materials [52–55]. As a result, the exploration of polymers tailored for specific applications has emerged as a central theme in the existing literature [56]. Deep learning is now helping to speed up noise removal in microscopy and improve phase processing in digital holography [57–61]. Many studies have also developed smart meta-surfaces that enable camouflage and radiative cooling, while machine learning techniques are being used to optimize laser drilling and fiber laser designs [62–66]. Other recent advances include hyperspectral image analysis, secure image steganography, and Bayesian optimization for better electromagnetic materials. A comprehensive review of optical fiber speckle sensing brings these developments together, showing how AI and photonics are becoming increasingly intertwined [67].

While our results demonstrate the potential of ML-based approaches for MMF systems, several limitations must be acknowledged. First, the experimental dataset (n = 225) is modest for deep learning applications, and the seven-case-study sample used for ANN demonstration represents a proof-of-concept rather than a fully validated model. The training/validation/test split (70/15/15%) yields only ~259 test samples, which limits the statistical power for detecting subtle performance differences. Second, the dataset was collected under controlled laboratory conditions; performance in field environments with additional noise sources and variable fiber conditions may differ. Third, the correlation between input parameters (r = 0.99 for mode coupling and dispersion) may lead to ill-conditioned models and spurious correlations; future work should explore orthogonal experimental designs to separate these effects. Fourth, the reported confidence intervals (width < 1.5% for ANN predictions) may be optimistic given the limited sample size. Despite these limitations, the quantitative framework and methodology presented here provide a foundation for future work with larger datasets and real-world validation.

Based on our findings, we identify five concrete research directions for advancing ML-assisted MMF systems: physics-guided data augmentation using energy conservation constraints to reduce experimental requirements by 60–70%; multi-task learning for simultaneous prediction of accuracy, mode composition, and dispersion, with 5–10% expected improvement; real-time adaptive control via reinforcement learning optimized for sub-1 ms response times; integrated photonic–ML systems utilizing optical convolutions to cut energy consumption by 90%; and systematic multi-fiber generalization testing across different core diameters and profiles to establish robust cross-fiber performance.

5. Conclusions

This study explored the use of machine learning to improve mode conversion and holographic reconstruction in multimode optical fiber systems, tackling three targeted research questions through both experimental data and physics-driven simulations. For RQ1, a proof-of-concept ANN analysis based on seven case-study samples uncovered a very strong correlation (r = 0.99) between mode coupling and intermode dispersion, with both factors substantially influencing reconstruction accuracy and producing prediction errors between

3.2% and 5.3% on test data—although the authors caution that these encouraging results must be corroborated with larger datasets before any claims of broad predictive reliability can be justified. In addressing RQ2, the CNN model achieved 93.7% classification accuracy on the held-out test set (n = 258 samples), cutting the mode error rate by 62% relative to conventional reconstruction techniques while preserving the SSIM above 0.85 even under low-SNR conditions (10 dB), thereby confirming that CNN-based methods can significantly outperform traditional digital signal processing in mode-separation tasks. Turning to RQ3, hybrid models that integrated physical constraints—such as energy conservation and phase stability—yielded encouraging preliminary outcomes, with an SSIM of 0.94 versus 0.91 for the standard CNN, hinting that incorporating domain knowledge may enhance generalization across diverse operational scenarios. The study's main contributions are threefold: establishing a quantitative framework for understanding parameter interdependencies in MMF systems, providing a rigorous comparison between CNN-based mode separation and non-ML benchmarks, and pioneering hybrid learning strategies to boost hologram fidelity. Nevertheless, several limitations must be acknowledged, including the relatively small experimental sample (n = 225), the preliminary nature of the ANN analysis, the controlled lab environment that may produce overoptimistic confidence intervals, and the fact that reinforcement learning and GNN approaches remain conceptual proposals rather than fully implemented solutions. To build on this foundation, subsequent research should concentrate on validating these methods with more extensive experimental datasets, deploying reinforcement learning for real-time adaptive control, incorporating optical convolutions to lower energy consumption, and conducting systematic evaluations across varied fiber types to ensure consistent performance. Ultimately, this work lays solid groundwork for ML-assisted MMF systems, showcasing their potential while transparently addressing existing shortcomings, and offers a reproducible methodology that can steer future efforts toward real-world deployment in advanced communication and imaging applications.

Funding: This work was supported by the UCL, Electronic and Electrical Engineering, London, project.

Data Availability Statement: The datasets supporting the conclusions of this study are included within the article.

Conflicts of Interest: The authors declare no conflicts of interest.

Abbreviations

AI	Artificial Intelligence
ANN	Artificial Neural Network
BPM	Beam Propagation Method
CNN	Convolutional Neural Network
DSP	Digital Signal Processing
DWDM	Dense Wavelength Division Multiplexing
FDTD	Finite-Difference Time-Domain
GAN	Generative Adversarial Network
GNN	Graph Neural Network
IoT	Internet of Things
ISI	Intersymbol Interference
LAN	Local Area Network
MER	Mode Error Rate
MCF	Multicore Fiber
ML	Machine Learning
MMF	Multimode Optical Fiber
NRMSE	Normalized Root Mean Square Error

PDM	Polarization Division Multiplexing
PINN	Physics-Informed Neural Network
PMD	Polarization Mode Dispersion
PSNR	Peak Signal-to-Noise Ratio
RL	Reinforcement Learning
RNN	Recurrent Neural Network
SAR	Specific Absorption Rate
SDM	Spatial Division Multiplexing
SDN	Software-Defined Networking
SLM	Spatial Light Modulator
SMF	Single-Mode Fiber
SNR	Signal-to-Noise Ratio
SSIM	Structural Similarity Index
TDM	Time Division Multiplexing
WDM	Wavelength Division Multiplexing

References

1. Wu, Q.; Qu, Y.; Liu, J.; Yuan, J.; Wan, S.P.; Wu, T.; Farrell, G. Singlemode-multimode-singlemode fiber structures for sensing applications—A review. *IEEE Sens. J.* **2020**, *21*, 12734–12751.
2. Ho, K.P.; Kahn, J.M.; Kaminow, I.P.; Li, T.; Willner, A.E. Mode coupling and its impact on spatially multiplexed systems. *Opt. Fiber Telecommun. VI* **2013**, *17*, 1386–1392.
3. Fu, B.; Shang, C.; Liu, H.; Fan, S.; Zhao, K.; Zhang, Y.; Wageh, S.; Al-Ghamdi, A.; Wang, X.; Xu, L.; et al. Recent advances and future outlook in mode-locked lasers with multimode fibers. *Appl. Phys. Rev.* **2023**, *10*, 041305. [CrossRef]
4. Su, Y.; He, Y.; Chen, H.; Li, X.; Li, G. Perspective on mode-division multiplexing. *Appl. Phys. Lett.* **2021**, *118*, 200502. [CrossRef]
5. Matsushima, K.; Arima, Y.; Nakahara, S. Digitized holography: Modern holography for 3D imaging of virtual and real objects. *Appl. Opt.* **2011**, *50*, H278–H284. [CrossRef] [PubMed]
6. Birdi, J.; Rajora, S.; Butola, M.; Khare, K. True 3D reconstruction in digital holography. *J. Phys. Photonics* **2020**, *2*, 044004. [CrossRef]
7. Butime, J.; Gutierrez, I.; Corzo, L.G.; Espronceda, C.F. 3D reconstruction methods, a survey. In *Proceedings of the First International Conference on Computer Vision Theory and Applications*; INSTICC: Lisboa, Portugal, 2006; pp. 457–463.
8. Zhang, Y.; Poon, T.C.; Tsang, P.W.; Wang, R.; Wang, L. Review on feature extraction for 3-D incoherent image processing using optical scanning holography. *IEEE Trans. Ind. Inform.* **2019**, *15*, 6146–6154. [CrossRef]
9. Kim, S.; Kim, D.D.; Anthony, B.W. Dynamic control of a fiber manufacturing process using deep reinforcement learning. *IEEE/ASME Trans. Mechatron.* **2021**, *27*, 1128–1137. [CrossRef]
10. Nevin, J.W.; Nallaperuma, S.; Shevchenko, N.A.; Li, X.; Faruk, M.S.; Savory, S.J. Machine learning for optical fiber communication systems: An introduction and overview. *APL Photonics* **2021**, *6*, 121101. [CrossRef]
11. Cao, D.; Zhao, J.; Hu, W.; Yu, N.; Ding, F.; Huang, Q.; Chen, Z. Deep reinforcement learning enabled physical-model-free two-timescale voltage control method for active distribution systems. *IEEE Trans. Smart Grid* **2021**, *13*, 149–165.
12. Liu, D.; Yang, Y.; Chen, X.; Ling, T.; Zhang, L.; Bai, J.; Shen, Y. Recent developments of interferometric wavefront sensing. In *Proceedings of the 2015 International Conference on Optical Instruments and Technology: Optoelectronic Measurement Technology and Systems*; SPIE: Bellingham, WA, USA, 2015; Volume 9623, pp. 9–18.
13. Wu, Y.; Sharma, M.K.; Veeraraghavan, A. WISH: Wavefront imaging sensor with high resolution. *Light Sci. Appl.* **2019**, *8*, 44. [CrossRef] [PubMed]
14. Zhang, Y.; An, Q.; Yang, M.; Ma, L.; Wang, L. A Review of Wavefront Sensing and Control Based on Data-Driven Methods. *Aerospace* **2025**, *12*, 399. [CrossRef]
15. Shariati, B.; Mastropaolo, A.; Diamantopoulos, N.P.; Rivas-Moscoso, J.M.; Klonidis, D.; Tomkos, I. Physical-layer-aware performance evaluation of SDM networks based on SMF bundles, MCFs, and FMFs. *J. Opt. Commun. Netw.* **2018**, *10*, 712–722. [CrossRef]
16. Karniadakis, G.E.; Kevrekidis, I.G.; Lu, L.; Perdikaris, P.; Wang, S.; Yang, L. Physics-informed machine learning. *Nat. Rev. Phys.* **2021**, *3*, 422–440. [CrossRef]
17. Cuomo, S.; Di Cola, V.S.; Giampaolo, F.; Rozza, G.; Raissi, M.; Piccialli, F. Scientific machine learning through physics–informed neural networks: Where we are and what's next. *J. Sci. Comput.* **2022**, *92*, 88. [CrossRef]
18. Leon-Saval, S.G.; Birks, T.A.; Bland-Hawthorn, J.; Englund, M. Multimode fiber devices with single-mode performance. *Opt. Lett.* **2005**, *30*, 2545–2547. [CrossRef] [PubMed]

19. Yin, B.; Li, Y.; Liu, Z.B.; Feng, S.; Bai, Y.; Xu, Y.; Jian, S. Investigation on a compact in-line multimode-single-mode-multimode fiber structure. *Opt. Laser Technol.* **2016**, *80*, 16–21. [CrossRef]
20. Caravaca-Aguirre, A.M.; Piestun, R. Single multimode fiber endoscope. *Opt. Express* **2017**, *25*, 1656–1665. [CrossRef] [PubMed]
21. Wang, K.; Dong, X.; Köhler, M.H.; Kienle, P.; Bian, Q.; Jakobi, M.; Koch, A.W. Advances in optical fiber sensors based on multimode interference (MMI): A review. *IEEE Sens. J.* **2020**, *21*, 132–142. [CrossRef]
22. Gao, C.; Cao, B.; Ding, Y.; Xiao, X.; Yang, D.; Fei, H.; Yang, C.; Bao, C. All-step-index-fiber spatiotemporally mode-locked laser. *Optica* **2023**, *10*, 356–363. [CrossRef]
23. Li, H.; Brio, M.; Li, L.; Schülzgen, A.; Peyghambarian, N.; Moloney, J.V. Multimode interference in circular step-index fibers studied with the mode expansion approach. *J. Opt. Soc. Am. B* **2007**, *24*, 2707–2720. [CrossRef]
24. Shemirani, M.B.; Mao, W.; Panicker, R.A.; Kahn, J.M. Principal modes in graded-index multimode fiber in presence of spatial-and polarization-mode coupling. *J. Light. Technol.* **2009**, *27*, 1248–1261. [CrossRef]
25. Girgis, L.; Milovic, D.; Konar, S.; Yildirim, A.; Jafari, H.; Biswas, A. Optical Gaussons in birefringent fibers and DWDM systems with intermodal dispersion. *Rom. Rep. Phys.* **2012**, *64*, 663–671.
26. Mohapatra, H.; Hosain, S.I. Intermodal dispersion free few-mode (quadruple mode) fiber: A theoretical modelling. *Opt. Commun.* **2013**, *305*, 267–270. [CrossRef]
27. Das, S.P. Mode-coupling theory and the glass transition in supercooled liquids. *Rev. Mod. Phys.* **2004**, *76*, 785–851. [CrossRef]
28. Yu, H.; Park, J.; Lee, K.; Yoon, J.; Kim, K.; Lee, S.; Park, Y. Recent advances in wavefront shaping techniques for biomedical applications. *Curr. Appl. Phys.* **2015**, *15*, 632–641. [CrossRef]
29. Horstmeyer, R.; Ruan, H.; Yang, C. Guidestar-assisted wavefront-shaping methods for focusing light into biological tissue. *Nat. Photonics* **2015**, *9*, 563–571. [CrossRef] [PubMed]
30. Xu, J.; Ruan, H.; Liu, Y.; Zhou, H.; Yang, C. Focusing light through scattering media by transmission matrix inversion. *Opt. Express* **2017**, *25*, 27234–27246. [CrossRef] [PubMed]
31. Van Zelst, A.; Van Nee, R.; Awater, G.A. Space division multiplexing (SDM) for OFDM systems. In *Proceedings of the VTC2000-Spring. 2000 IEEE 51st Vehicular Technology Conference Proceedings (Cat. No. 00CH37026)*; IEEE: New York, NY, USA, 2000; Volume 2, pp. 1070–1074.
32. Puttnam, B.J.; Rademacher, G.; Luís, R.S. Space-division multiplexing for optical fiber communications. *Optica* **2021**, *8*, 1186–1203. [CrossRef]
33. Saridis, G.M.; Alexandropoulos, D.; Zervas, G.; Simeonidou, D. Survey and evaluation of space division multiplexing: From technologies to optical networks. *IEEE Commun. Surv. Tutor.* **2015**, *17*, 2136–2156. [CrossRef]
34. Li, G.; Bai, N.; Zhao, N.; Xia, C. Space-division multiplexing: The next frontier in optical communication. *Adv. Opt. Photonics* **2014**, *6*, 413–487. [CrossRef]
35. van Zelst, A. Space division multiplexing algorithms. In *Proceedings of the 2000 10th Mediterranean Electrotechnical Conference. Information Technology and Electrotechnology for the Mediterranean Countries. Proceedings. MeleCon 2000 (Cat. No. 00CH37099)*; IEEE: New York, NY, USA, 2000; Volume 3, pp. 1218–1221.
36. Cheben, P.; Xu, D.X.; Janz, S.; Densmore, A. Subwavelength waveguide grating for mode conversion and light coupling in integrated optics. *Opt. Express* **2006**, *14*, 4695–4702. [CrossRef] [PubMed]
37. Fang, Q.; Liow, T.Y.; Song, J.F.; Tan, C.W.; Yu, M.B.; Lo, G.Q.; Kwong, D.L. Suspended optical fiber-to-waveguide mode size converter for silicon photonics. *Opt. Express* **2010**, *18*, 7763–7769. [CrossRef] [PubMed]
38. Velasco-Garcia, M.N.; Mottram, T. Biosensor technology addressing agricultural problems. *Biosyst. Eng.* **2003**, *84*, 1–12. [CrossRef]
39. Tong, X.C. Fundamentals and design guides for optical waveguides. In *Advanced Materials for Integrated Optical Waveguides*; Springer: Berlin/Heidelberg, Germany, 2013; pp. 1–51.
40. Khonina, S.N.; Kazanskiy, N.L.; Skidanov, R.V.; Butt, M.A. Exploring types of photonic neural networks for imaging and computing—A review. *Nanomaterials* **2024**, *14*, 697. [CrossRef] [PubMed]
41. Tsui, H.C.L.; Sirbu, D.; Alsaif, N.; Hill, N.; Tizzard, G.; Docampo, P.; Healy, N. Few-mode metal-free perovskite optical fiber with second-order optical nonlinearity. *APL Photonics* **2024**, *9*, 036106. [CrossRef]
42. Schnars, U.; Falldorf, C.; Watson, J.; Jüptner, W. *Digital Holography*; Springer: Berlin/Heidelberg, Germany, 2015; pp. 39–68.
43. Wang, J.; Ilyas, N.; Ren, Y.; Ji, Y.; Li, S.; Li, C.; Liu, F.; Gu, D.; Ang, K.W. Technology and integration roadmap for optoelectronic memristor. *Adv. Mater.* **2024**, *36*, 2307393. [CrossRef]
44. Chauhan, N.K.; Singh, K. A review on conventional machine learning vs deep learning. In *Proceedings of the 2018 International Conference on Computing, Power and Communication Technologies (GUCON)*; IEEE: New York, NY, USA, 2018; pp. 347–352.
45. Gupta, J.; Pathak, S.; Kumar, G. Deep learning (CNN) and transfer learning: A review. *J. Phys. Conf. Ser.* **2022**, *2273*, 012029. [CrossRef]
46. Rahmani, F.; Barbaz-Isfahani, R.; Saber-Samandari, S.; Salehi, M. Experimental and analytical investigation on forced and free vibration of sandwich structures with reinforced composite faces in an acidic environment. *Heliyon* **2023**, *9*, e20864. [CrossRef] [PubMed]

47. Dadras, H.; Teimouri, A.; Barbaz-Isfahani, R.; Saber-Samandari, S. Indentation, finite element modeling and artificial neural network studies on mechanical behavior of GFRP composites in an acidic environment. *J. Mater. Res. Technol.* **2023**, *24*, 5042–5058. [CrossRef]
48. Gitiara, Y.; Barbaz-Isfahani, R.; Saber-Samandari, S.; Sadighi, M. Low-velocity impact behavior of incorporated GFRP composites with nanoclay and nanosilica in a corrosive environment: Experimental and numerical study. *J. Compos. Mater.* **2021**, *55*, 3989–4010. [CrossRef]
49. Barbaz-Isfahani, R.; Khalvandi, A.; Tran, T.M.N.; Kamarian, S.; Saber-Samandari, S.; Song, J.I. Synergistic effects of egg shell powder and halloysite clay nanotubes on the thermal and mechanical properties of abacá/polypropylene composites. *Ind. Crops Prod.* **2023**, *205*, 117498. [CrossRef]
50. Rahmani, F.; Barbaz-Isfahani, R.; Saber-Samandari, S.; Salehi, M. Effect of corrosive environment on mechanical properties of polymer-based nanocomposite: Analytical and experimental study. *Mater. Today Commun.* **2023**, *36*, 106544. [CrossRef]
51. Kamarian, S.; Khalvandi, A.; Tran, T.M.N.; Barbaz-Isfahani, R.; Saber-Samandari, S.; Song, J.I. Predicting ESP and HNT effects on the mechanical properties of eco-friendly composites subjected to micro-indentation test. *JAinr* **2023**, *15*, 315–328.
52. Barbaz-Isfahani, R.; Dadras, H.; Saber-Samandari, S.; Taherzadeh-Fard, A.; Liaghat, G. A comprehensive investigation of the low-velocity impact response of enhanced GFRP composites with single and hybrid loading of various types of nanoparticles. *Heliyon* **2023**, *9*, e15930. [CrossRef] [PubMed]
53. Alimirzaei, S.; Barbaz-Isfahani, R.; Khodaei, A.; Najafabadi, M.A.; Sadighi, M. Investigating the flexural behavior of nanomodified multi-delaminated composites using acoustic emission technique. *Ultrasonics* **2024**, *138*, 107249. [CrossRef] [PubMed]
54. Barbaz-Isfahani, R.; Dadras, H.; Taherzadeh-Fard, A.; Zarezadeh-Mehrizi, M.A.; Saber-Samandari, S.; Salehi, M.; Liaghat, G. Synergistic effects of incorporating various types of nanoparticles on tensile, flexural, and quasi-static behaviors of GFRP composites. *Fibers Polym.* **2022**, *23*, 2003–2016. [CrossRef]
55. Barbaz-Isfahani, R.; Saber-Samandari, S.; Salehi, M. Experimental and numerical research on healing performance of reinforced microcapsule-based self-healing polymers using nanoparticles. *J. Reinf. Plast. Compos.* **2023**, *42*, 95–109.
56. Sun, G.; Sheng, L.; Luo, L.; Yu, H. Game Theoretic Approach for Multipriority Data Transmission in 5G Vehicular Networks. *IEEE Trans. Intell. Transp. Syst.* **2022**, *23*, 24672–24685. [CrossRef]
57. Yu, X.; Luan, S.; Lei, S.; Huang, J.; Liu, Z.; Xue, X.; Zhu, B. Deep learning for fast denoising filtering in ultrasound localization microscopy. *Phys. Med. Biol.* **2023**, *68*, 205002. [CrossRef]
58. Zhou, G.; Huang, J.; Li, H.; Li, Y.; Jia, G.; Song, N.; Xiao, J. Multispectral camouflage and radiative cooling using dynamically tunable metasurface. *Opt. Express* **2024**, *32*, 12926–12940. [CrossRef] [PubMed]
59. Wang, C.; Zhang, Z.; Jing, X.; Yang, Z.; Xu, W. Optimization of multistage femtosecond laser drilling process using machine learning coupled with molecular dynamics. *Opt. Laser Technol.* **2022**, *156*, 108442. [CrossRef]
60. Zhang, Z.; Yang, Z.; Wang, C.; Xu, W. Accelerating ultrashort pulse laser micromachining process comprehensive optimization using a machine learning cycle design strategy integrated with a physical model. *J. Intell. Manuf.* **2024**, *35*, 449–465.
61. Zhang, Z.; Liu, S.; Zhang, Y.; Wang, C.; Zhang, S.; Yang, Z.; Xu, W. Optimization of low-power femtosecond laser trepan drilling by machine learning and a high-throughput multi-objective genetic algorithm. *Opt. Laser Technol.* **2022**, *148*, 107688. [CrossRef]
62. Ma, W.; Li, X.; Qin, Y.; Chen, W.; Hu, G. High-power spatiotemporal mode-locked Yb-doped fiber laser based on transverse modes division control. *Opt. Lett.* **2025**, *50*, 5202–5205. [CrossRef] [PubMed]
63. Tu, B.; Zhou, T.; Liu, B.; He, Y.; Li, J.; Plaza, A. Multi-scale autoencoder suppression strategy for hyperspectral image anomaly detection. *IEEE Trans. Image Process.* **2025**, *34*, 5115–5130. [CrossRef] [PubMed]
64. Wenbo, J.; Lirui, L.; Yun, B. Application of deep learning in the phase processing of digital holographic microscopy. *Photonics* **2025**, *12*, 810. [CrossRef]
65. Luo, T.; Zhou, Y.; He, Z.; Jiang, G.; Xu, H.; Qi, S.; Zhang, Y. StegMamba: Distortion-free immune-cover for multi-image steganography with state space model. *IEEE Trans. Circuits Syst. Video Technol.* **2024**, *35*, 4576–4591.
66. Yang, N.; Gao, H.; Ju, S.; Zhang, Z.; Zhao, Y.; Guo, X.W.; Xing, S.; Liu, J.; Zhang, J.; Duan, K.; et al. Achieving broadband electromagnetic absorption in laminated composites through progressive Bayesian optimization. *Compos. Part B Eng.* **2025**, *307*, 112882. [CrossRef]
67. Chapalo, I.; Stylianou, A.; Mégret, P.; Theodosiou, A. Advances in optical fiber speckle sensing: A comprehensive review. *Photonics* **2024**, *11*, 299. [CrossRef]

Disclaimer/Publisher's Note: The statements, opinions and data contained in all publications are solely those of the individual author(s) and contributor(s) and not of MDPI and/or the editor(s). MDPI and/or the editor(s) disclaim responsibility for any injury to people or property resulting from any ideas, methods, instructions or products referred to in the content.